LWA-OVRO Memo No. 8

Filter Designs for Next-Generation Analog Receivers

Larry D'Addario and Nitika Marwaha
California Institute of Technology

2019 August 19

Including copies of these prior design reports

ARX Filter Selection

2019 July 15

Proposed Filters For Next-Generation Analog Receivers

2019 May 2

Submitted 2020 June 2

Filter Designs for Next-Generation Analog Receivers

Larry R. D'Addario
California Institute of Technology
2019 August 19

I. Introduction

A preliminary design for bandpass filters in the next-generation analog receivers of OVRO-LWA is described in [3] and was presented at the Preliminary Design Review of June 2019. The plan was to provide three remotely-selectable filters, all of which are intended to suppress high-power RFI in the bands below 20 MHz and above 88 MHz. One filter ("Wide") extends the bandwidth as much as practical on each end, while accepting some risk that observations will be RFI-contaminated or that gain and SNR will have to be reduced to avoid intermodulation. Another ("Safe") is intended to have low risk of RFI contamination and to maximize sensitivity in the center of the observing band, while accepting lower total bandwidth. The third ("Smooth") is designed to have a maximally-smooth bandpass, requiring still smaller total bandwidth to achieve adequate RFI suppression. The designs included selection of specific, available components and detailed simulations of performance, taking into account non-ideal behavior of practical inductors and parasitic effects of PC board layout.

Since then, additional studies have been done via simulation of the performance of the selected filters in the measured RFI environment at OVRO, and some adjustments to the cutoff frequencies have been explored. This is partly in response to a suggestion in the PDR report of the Technical Advisory Committee [2] that frequency coverage be extended to lower frequencies than had previously been considered. This has led to changes in the filter selection topology and in the details of the filter responses. This memo describes the current design ("ARX filters revision 2") and the considerations that led to it.

The new designs include specific component selection and detailed simulation, and they have been implemented on a test printed circuit board. Results of simulations and testing are reported here.

II. Design Considerations

A. Topology

The sharpness of cutoff (and consequently filter complexity) required at the low-frequency end of the band is much less than that required at the high-frequency end. This is partly because RFI is much stronger above 88 MHz than below 20 MHz, but also because a given transition band width is a smaller fraction of the cutoff frequency at high frequencies than at low frequencies. This makes it efficient to implement each bandpass filter as a cascade of a lowpass and highpass filter. This technique was used for the Wide and Safe filters of the preliminary design. In that case, rather than providing three selectable filters, more flexibility is obtained by providing two selectable lowpass filters and two independently-selectable highpass filters, giving a total of four possible combinations as shown in Figure 1. That configuration has now been adopted. (The selection of filter cutoff frequencies is discussed below.)

It was realized that the Smooth filter is not necessary. In view of the spectral resolution of the LWA's signal processing (24 kHz), the smoothness of even steep-cutoff elliptical-response filters is sufficient. For example, Figure 2 shows the response of the two sharpest-cutoff filters of the preliminary-design, including the group delays. The peak group delay of $\tau = 46$ ns occurs for the Safe filter, which uses a 9th-order Chebyshev lowpass, That corresponds to a phase slope of $d\varphi/df = 2\pi\tau = 2.89\text{e-}7$ rad/Hz or 0.39° in 24 kHz. Thus the 24 kHz frequency resolution of the

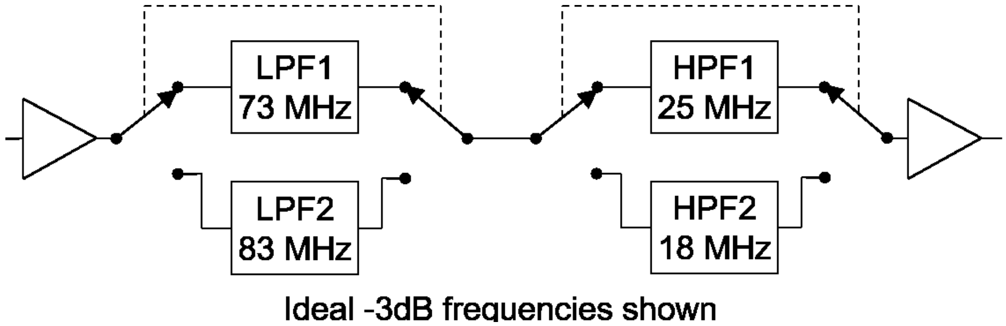

Figure 1. New filter selection topology. Either of the two lowpass and either of the two highpass filters can be independently selected, allowing four combinations.

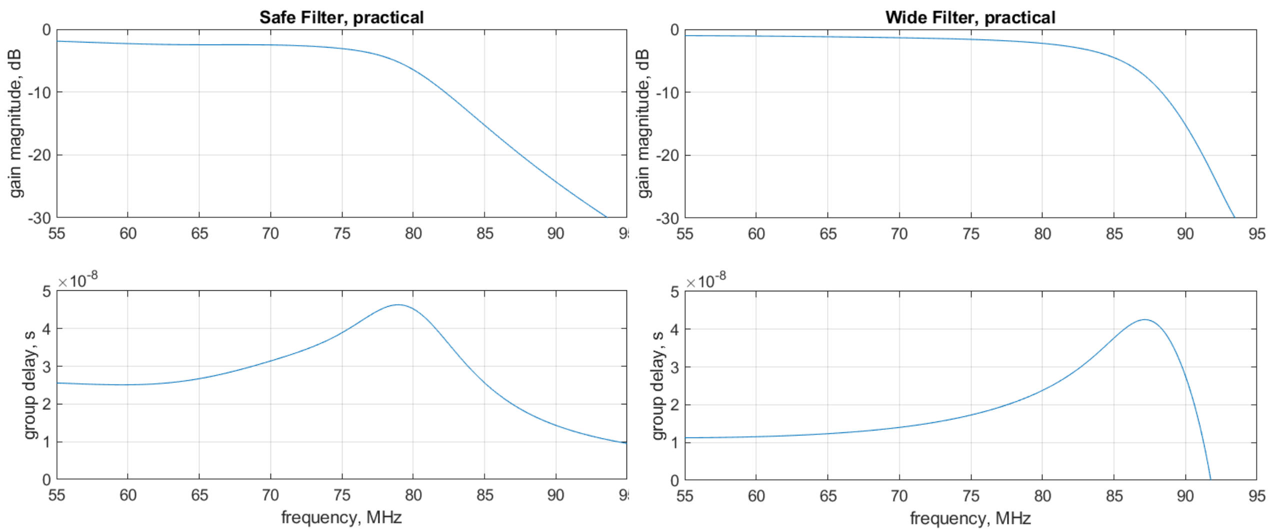

Figure 2. Simulated responses of two filters of the preliminary design near the high frequency cutoffs, where the gain change is sharpest. Both the gain magnitude and group delay are shown. In spite of the sharpness, the group delay variation is sufficiently smooth.

LWA tracks the phase variation very accurately. Furthermore, for interferometry, only the difference in delay between pairs of signals is important, and the filters are expected to be matched within about 5% (1% or 2% component tolerances and identical layouts).

The filter choices are made difficult by the intension that this telescope will mostly be used commensally, with multiple science programs processing the same signals. There will thus be one selection that is used most of the time and that must provide sufficient suppression of both low-end and high-end RFI to avoid intermodulation and clipping while still providing as much useful bandwidth as possible.

The multiple options are not intended to support different kinds of observing, although they could be used in that way if necessary; rather, they are intended to mitigate the risk that we will not choose the commensal-observing filter correctly. There is some uncertainty about the RFI environment, and there is uncertainty about how much intermodulation and clipping are tolerable, especially for mid-band observations of maximum sensitivity. The LPF1/HPF1 pair is reasonably expected to provide sufficient RFI immunity, but it is possible that one or more of the other options will also be sufficient, in which case we will be able to support certain high-frequency and low-frequency science at the same time as sensitive mid-band science.

B. Upper Cutoff Frequency and Sharpness (Lowpass Filters)

At the high-frequency end of the band, we have strong FM radio RFI beginning at 88 MHz and an especially strong local station at 92.5 MHz, yet there is a desire from the cosmic dawn science case to observe up to as high a frequency as possible; the formal requirement [1] is currently 83 MHz. That requires a very sharp cutoff, and it is not achieved by the preliminary-design's Safe filter [3], which uses a 9th-order Chebyshev lowpass and has a practical –3 dB frequency of 78.2 MHz. The 7th-order elliptical lowpass of the Wide design gets to 84.4 MHz at –3 dB, according to simulations. All of the preliminary-design filters were chosen to have about –20 dB attenuation at 88 MHz.

In the new design, the same 9th-order Chebyshev (0.1 dB max passband loss) will be retained as one of the LPF selections (LPF1) to ensure that we have one option with high attenuation throughout the FM band and higher (the FEE response extends to about 150 MHz). The other LPF will be a 7th-order elliptical, allowing very steep cutoff. Two designs are currently under consideration, both with nominal 0.1 dB passband ripple; the nominal –0.1 dB cutoffs are 82.2 MHz for the baseline (LPF2) and 85.0 MHz for the option. The simulated response of the baseline filter is below –30 dB throughout the FM radio band. The optional filter is more aggressive; it is only about –16 dB at 88 MHz, but is still below –30 dB over most of the FM band. Both are included on the filter test PCB, discussed later.

C. Lower Cutoff Frequency and Sharpness (Highpass Filters)

At the low-frequency end, the formal requirement [1] is currently 25 MHz (Jupiter science case), but the PDR report [2] suggested that we should consider pushing to lower frequencies. It turns out that 25 MHz is easy; the preliminary-design filters all have practical –3 dB cutoffs below 25 MHz. Here we take a closer look at the RFI suppression needed. (See Section V below for additional analysis and discussion.)

Figure 3 shows the measured 12h dynamic spectrum of a signal from a core antenna. No filtering was applied after the front end electronics (which includes only a 150 MHz LPF and slow roll-off below 10 MHz due to d.c. blocking capacitors). This shows that the RFI below 20 MHz is highly time-variable, so it can be expected that there are some periods of low RFI at

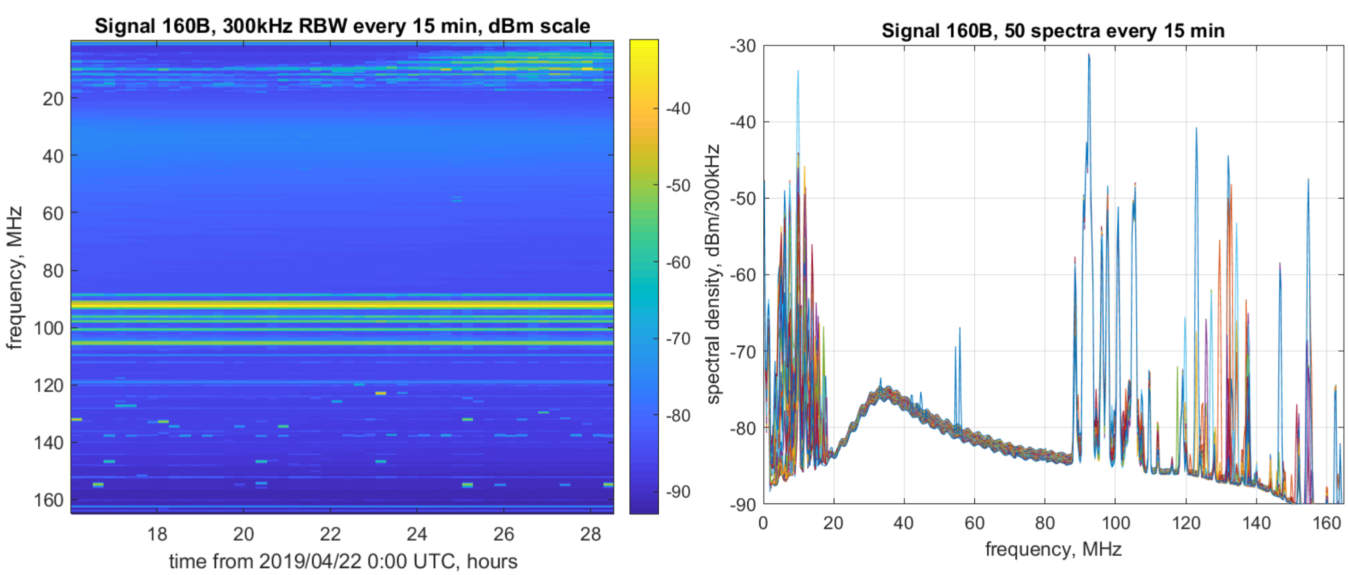

Figure 3. Dynamic spectrum of a signal from a core antenna with short coax length (0-165 MHz with 0.3MHz RBW, every 15m for ~12h), along with all spectra overlaid. No filtering preceding an Agilent spectrum analyzer. Similar to the results in [5]; see that report for details of the setup.

some frequencies.

Figure 4 (reproduced from [4]) shows that the LWA antennas are expected to have low sensitivity below 20 MHz. The radiation resistance and mismatch efficiency are nearly zero. In spite of the $f^{-2.55}$ frequency dependence of sky noise, the signal is not sky-noise-dominated; at 15 MHz it is about 75% receiver noise.

Even though the antenna sensitivity is much reduced below 20 MHz, the fact that we see substantial RFI (Fig. 3) implies that it has some sensitivity to signals from the sky (perhaps a few percent of that of an antenna tuned to that range). The actual sensitivity is somewhat uncertain because Fig. 4 is based on imperfect simulations, not field measurements.

In the new design, two 5th-order Butterworth filters will be used with practical –3 dB cutoffs of 20.5 and 26.5 MHz and –20 dB cutoffs of 12 and 16 MHz, respectively. The former is

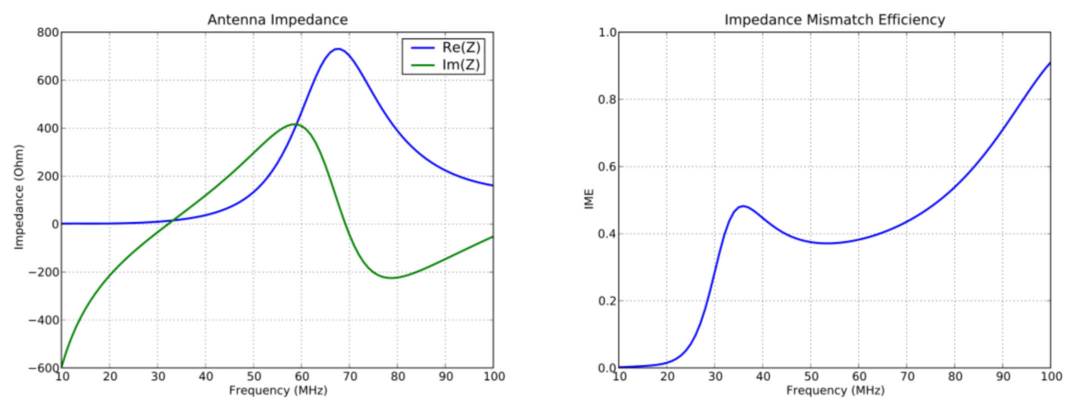

Figure 2.5: Antenna terminal impedance and impedance mismatch efficiency

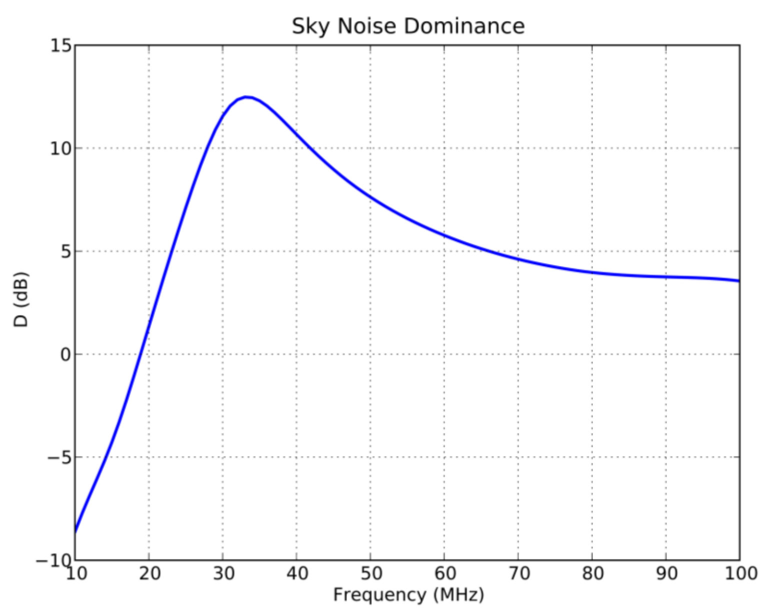

Figure 2.6: Predicted sky noise dominance (D) for ANT + GND as a function of frequency including impedance mismatch and ground losses calculated using NEC-4 and assuming T_{FEE} = 250 K and Z_{FEE} = 100 Ω. The Cane [16] model for sky noise at the Galactic pole is assumed, so this is a minimum sky noise dominance.

Figure 4. LWA antenna terminal impedance, mismatch efficiency, and sky noise dominance (system temperature/receiver temperature), from [4].

expected to allow observing down to about 15 MHz during times of low RFI; the latter allows observing to about 20 MHz while suppressing most of the RFI. Nevertheless, a third filter is being considered and is included on the test board; it has practical –3 dB cutoff at 16.2 MHz and would allow observing down to nearly 10 MHz. It would not suppress much of the <20 MHz RFI, but that RFI may be sufficiently low to be accommodated by the ADCs, at least some of the time. (See Section VI of this memo for a more quantitative study of the RFI suppression of each filter.)

Butterworth filters are not as sharp as the Chebyshev filters used in the preliminary design, but the selected cutoffs provide sufficient RFI suppression. The Butterworth type is chosen here for the highpass filters because of the cascading with the sharper lowpass filters. To obtain sufficient sharpness, the latter allow 0.1 dB ripple in their passbands, which means that they have peak reflection coefficients of –16.4 dB at a few frequencies. To avoid making the cascaded reflection coefficients worse, the no-ripple Butterworth designs are selected for the highpass filters.

III. Design Details

The design parameters of the filters and a summary of their simulated responses are listed in Table 1. The "ripple" values are the design maximum passband loss and minimum stopband loss. The "cuttoff" frequency is the passband edge (–3 dB for Butterworth and –0.1 dB for others).

Table 1: Filter Parameters and Simulation Summary

	Design Parameters				Simulated Response			
	Type	Order	Ripple dB	Cutoff MHz	Ideal, MHz		Practical, MHz	
					-3 dB	-20dB	-3 dB	-20dB
LPF1	Chebyshev	9	0.1/∞	73.0	76.1	84.0	75.8	85.5
LPF2	Elliptical	7	0.1/30	82.2	83.4	85.5	82.9	87.2
LPF option	Elliptical	7	0.1/30	85.0	86.1	88.4	83.5	89.3
HPF1	Butterworth	5	0/∞	24.6	24.6	15.6	25.2	15.5
HPF2	Butterworth	5	0/∞	18.2	18.2	11.7	18.7	11.5
HPF option	Butterworth	5	0/∞	14.9	14.9	9.5	15.5	9.8

Schematics of all filters, with ideal component values, are shown in Figure 5.

Practical components were selected from those readily available. Nominal values closest to the ideal ones were chosen. Capacitor values have 1% tolerance and inductors have 1% or 2% tolerance. Inductors are mostly 0805 size, which is enough to achieve reasonable Q while not using excessive board space. All capacitors are size 0402 and use NPO dielectric. In some cases it was necessary to use two capacitors in parallel to get a value close enough to the ideal one. Some capacitor values were adjusted with the help of the simulations to make the filter response closer to ideal; for example, the series LC resonators of the elliptical filters were moved close to the ideal resonant frequencies by adjusting the capacitor values to compensate for the difference between available and ideal inductor values. All selected inductors have self-resonant frequencies well above our passband; the lowest is 770 MHz (330 nH for HPF option).

The selected component values are given in Table 2, along with manufacturer and part number. All inductors are from Coilcraft. For each capacitor, an acceptable manufacturer and part number are given, but in most cases an equivalent product is available from other manufacturers.

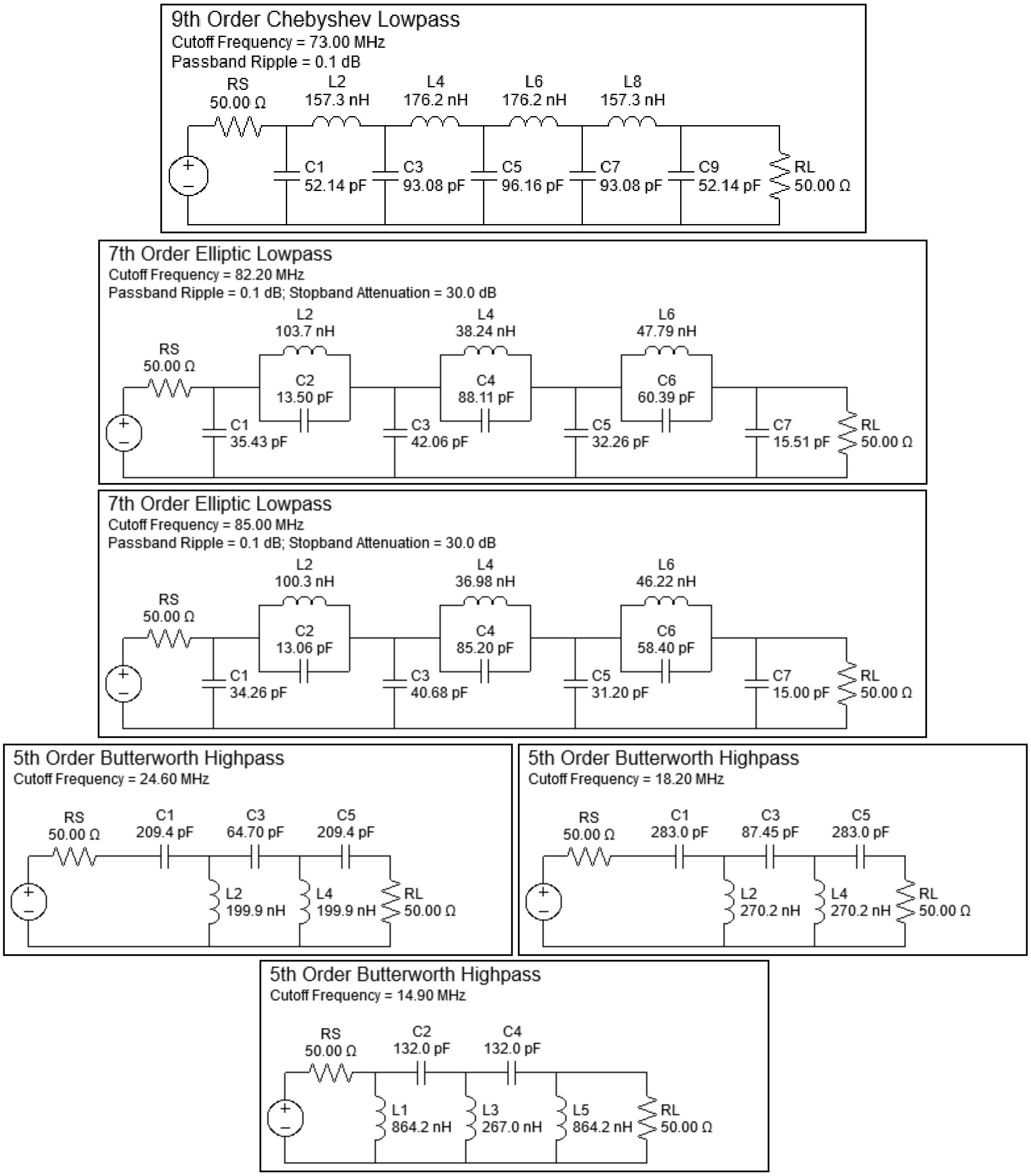

Figure 5. Filter schematics with ideal component values. Top to bottom: LPF1, LPF2, LPF option, HPF1 and HPF2, HPF option.

IV. Performance Analysis From Simulations

The designs have been simulated in LT Spice using the same methods as earlier [3]. For the inductors, manufacturer-supplied models were used. Capacitors were treated as ideal, which is reasonable for small ceramic capacitors at <100 MHz. Estimated PCB pad capacitances have been included in the simulations, using the smallest recommended dimensions or 0402, 0603, and 0805 devices and 0.22 mm thick FR4 over a ground plane. The pad capacitances had negligible effect on the results.

Table 2: Selected Components

LPF1 (C9 0.1 73.0)				LPF2 (E7 0.1/30 82.2)				LPF option (E7 0.1/30 85.0)			
Ref	Value	Mfgr	PN	Ref	Value	Mfgr	PN	Ref	Value	Mfgr	PN
C1,C9	56 pF	Yageo	CC0402FRNPO9BN560	C1	18+18 pF	Yageo	CC0402FRNPO9BN180	C1	33 pF	Yageo	CC0402FRNPO9BN330
L2,L8	150 nH	Coilcraft	0805CS-151XFEB	L2	100 nH	Coilcraft	0805HP-101XGEB	L2	100 nH	Coilcraft	0805HP-101XGEB
C3,C7	47+43 pF	Yageo	CC0402FRNPO9BN470	C2	14 pF	AVX	4025U140FAT2A	C2	13 pF	AVX	04025U130FAT2A
		KEMET	CBR04C430F5GAC	C3	27+15 pF	Yageo	CC0402FRNPO9BN270	C3	39 pF	Yageo	CC0402FRNPO9BN390
L4,L6	180 nH	Coilcraft	0805CS-181XFEB			Yageo	CC0402FRNPO9BN150	L4	36 nH	Coilcraft	0805CS-360XFEB
C5	47+47 pF	Yageo	CC0402FRNPO9BN470	L4	39 nH	Coilcraft	0805HP-101XGEB	C4	47+39 pF	Yageo	CC0402FRNPO9BN470
				C4	82 pF	Yageo	CC0402FRNPO9BN820			Yageo	CC0402FRNPO9BN390
				C5	33 pF	Murata	GCM1555C1H330FA16D	C5	30 pF	Murata	GJM1555C1H300FB01D
				L6	47 nH	Coilcraft	0805HP47NXGEB	L6	47 nH	Coilcraft	0805HP47NXGEB
				C6	62 pF	AVX	04025A620FAT2A	C6	56 pF	Yageo	CC0402FRNPO9BN560
				C7	15 pF	Yageo	CC0402FRNPO9BN150	C7	15 pF	Yageo	CC0402FRNPO9BN150
HPF1 (B5 24.6)				HPF2 (B6 18.2)				HPF option (B5 14.9)			
Ref	Value	Mfgr	PN	Ref	Value	Mfgr	PN	Ref	Value	Mfgr	PN
C1,C5	220 pF	Walsin	0402N221F500CT	C1,C5	270 pF	Murata	GCM1555C1H271FA16D	C1,C5	330 pF	Walsin	0402N331F500CT
L2,L4	200 nH	Coilcraft	0603HP-R20XGEU	L2,L4	270 nH	Coilcraft	0805HP-271XGRB	L2,L4	330 nH	Coilcraft	0805HP-331XGRB
C3	62 pF	AVX	04025A620FAT2A	C3	39 pF	Yageo	CC0402FRNPO9BN390	C3	56 pF	Yageo	CC0402FRNPO9BN560

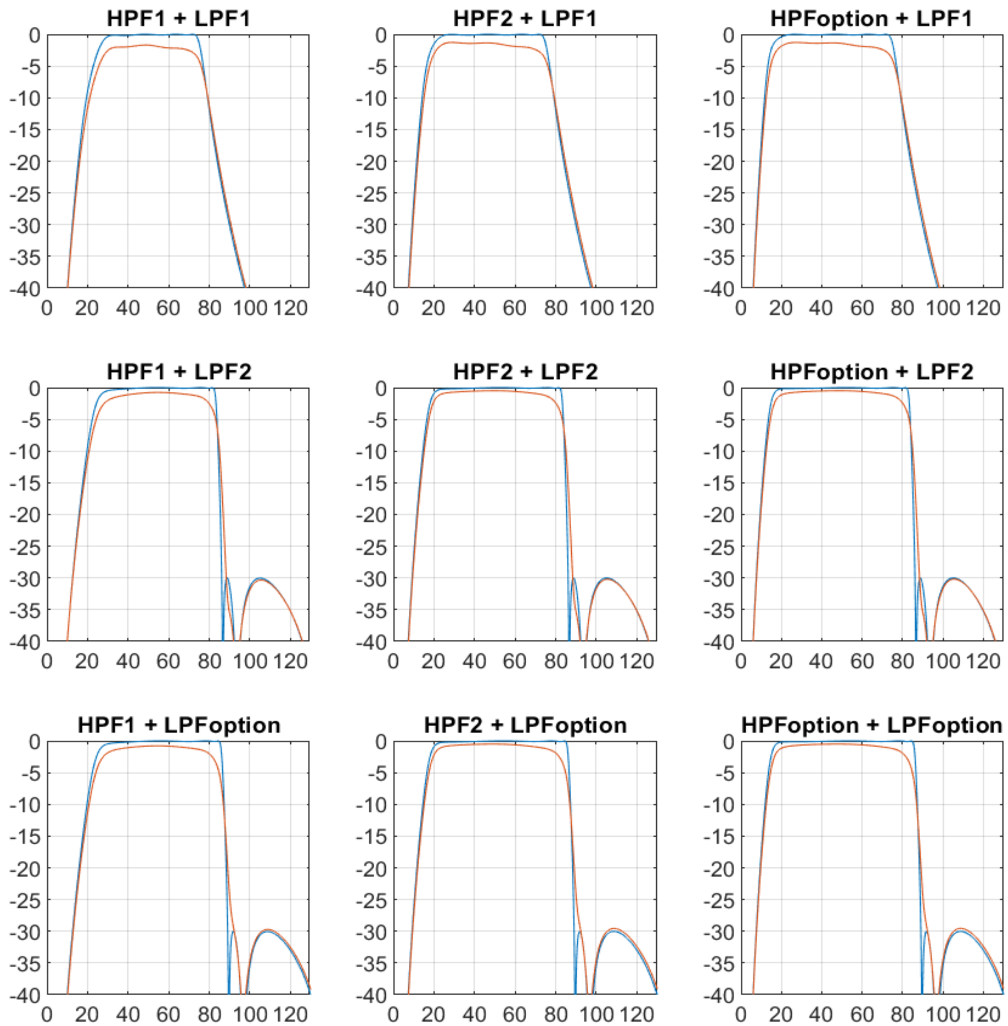

Figure 6. Simulated responses of highpass-lowpass cascades using all filters of Table 1, in dB, vs. frequeny in MHz. Blue is for ideal components (Fig 3) and red is for the actual components (Table 2) using inductor models from Coilcraft.

Using the 6 filters shown in Table 1, all 9 possible highpass-lowpass cascades were simulated. The magnitudes of the transfer functions are plotted in Figure 6. A subset of them, including all six filters of Table 1, is shown in more detail and further discussed in the next section. A file containing all the results, computed from 0 to 200 MHz every 0.1 MHz and including phase of the transfer functions, is available from the author on request.

V. Affect of Filters on RFI

The simulated responses shown in Fig. 6 have been used along with the dynamic spectrum measurements of signal 160B on 2019 Apr 22 (Fig. 3) to see how each of the nine filters would have affected that signal on that day.

Each measured spectrum was integrated to determine the total power in the low RFI band (< 20 MHz), the nominal observing band (25-85 MHz), and the high RFI band (> 88 MHz). Figure 7 is a time series of those total powers over the 12h of measurements. Without filtering, it is clear that there is far more power in the RFI bands than in the observing band. The power in the high RFI band, mainly FM radio, is stable, whereas the power in the low RFI band is highly time-variable. The observing band power shows the expected diurnal variation as a function of the height of the galactic plane in the visible sky.

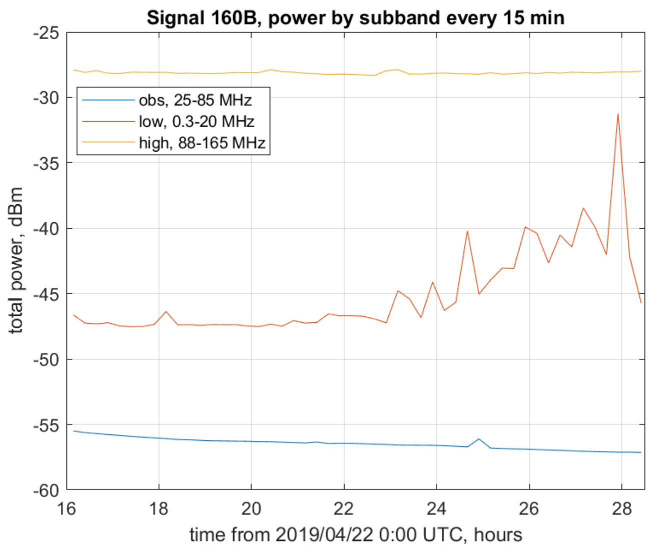

Figure 7. Time series of total power in each of three subbands, 0.3-20 MHz, 25-85 MHz, and 88-165 MHz, computed from the measured spectra from one core antenna shown in Fig. 3. See Fig. 8 for the effects of applying the filters to this signal.

The corresponding three time series after applying each filter to each measured spectrum are plotted in Figure 8. For all filters, both RFI bands have less power than the observing band most of the time. For the low RFI band, even the lowest-cutoff filter ("HPF option") keeps the RFI well below the observing band power for half of the observed time period and only 7 dB above at the worst time. For the high RFI band, the highest-cutoff filter ("LPF option") suppresses the RFI to about the same level as the observing band power. The other filters do about 3 dB better (LPF1) and 10 dB better (LPF2).

It might have been expected that the lowest-cutoff high-frequency filter (LPF1) would provide the largest RFI suppression. Even though its Chebychev 9th order design does not have as sharp a cutoff as the elliptical 7th order design of the others, its stopband begins at a lower frequency (76 MHz at –3 dB vs. 83-84 MHz) and its attenuation increases monotonically with frequency. The observed results occur because the high-frequency RFI is dominated by a single FM radio station centered at 92.5 MHz (KSRW, 185 W to an antenna on a 233m high tower in Independence, CA). That frequency is near one of the nulls in the response of LPF2. If the high-band RFI spectrum changes in the future, especially if new RFI sources arise at higher frequencies, then LPF1 could easily become the most effective of the three.

Which filters are acceptable and the choice of those to use in the new ARX design are

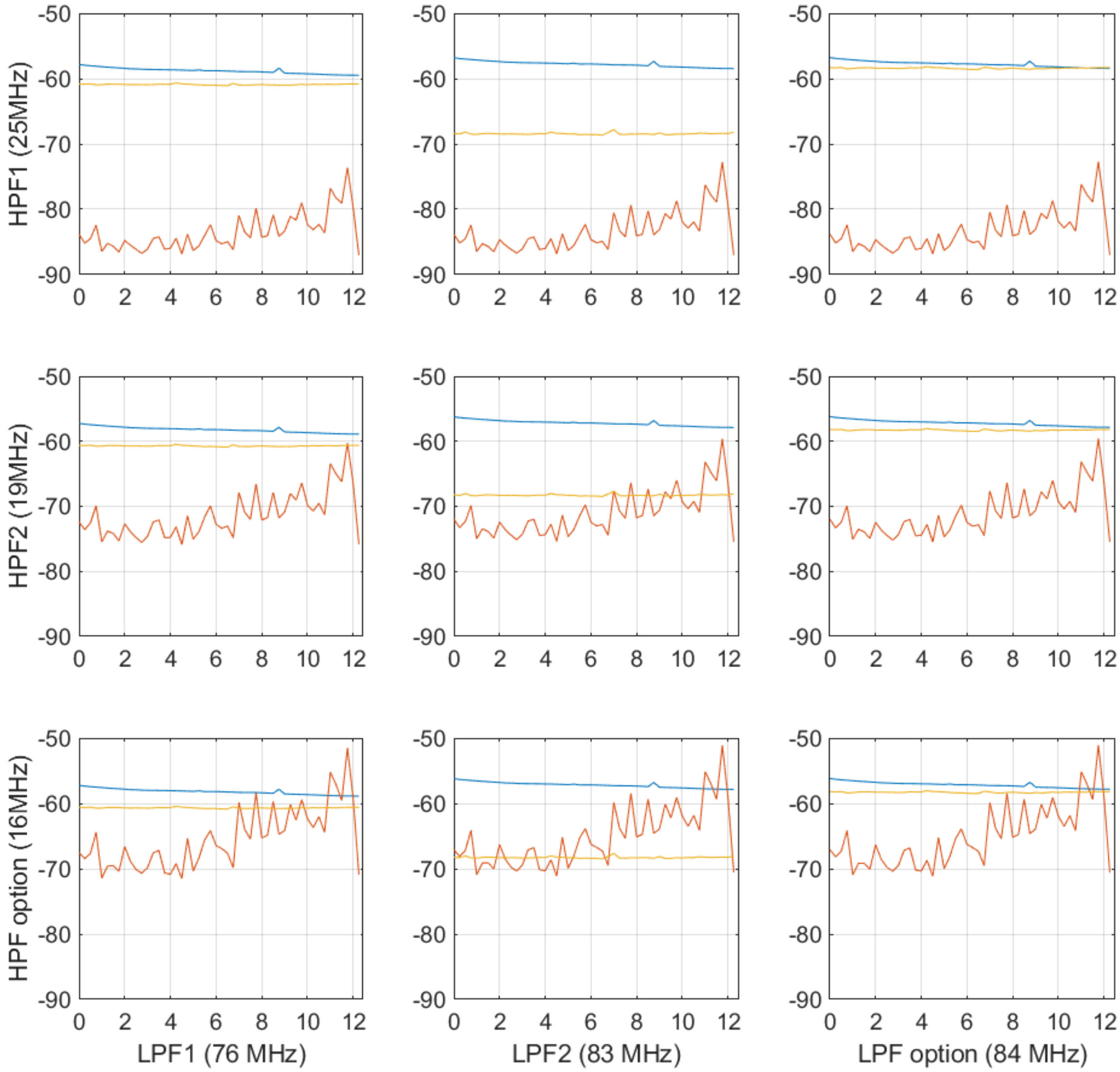

Figure 8. Time series of total power in observing band and RFI bands after applying the simulated filters (Fig. 3) to the measured spectra. For each subplot, the abscissa is time in hours from 16:09 UTC 22-Apr-2019, and the ordinate is total power in dBm. Compare with the corresponding unfiltered time series in Fig. 7. Each row is a different low frequency HPF and each column is a different high frequency LPF from Table 1; the –3 dB frequencies from the simulations are given.

discussed in Section VII below.

VI. Filter Test Board and Measurements

A printed circuit board containing three bandpass filters designed and fabricated, as shown in Figure 9. Each filter is a cascade of one HPF from Table 1 (left side of photo), a small attenuator (2dB or 3dB), and one LPF from Table 1, all using the components from Table 2. Each filter is implemented twice, first with a loose layout (components well separated, top of photo) and then with a compact layout (bottom of photo). The filters are (top to bottom):

- "Safe": HPF1 (24.6 MHz), 2 dB pad, LPF1 (76 MHz)
- "Wide": HPF option (14.9 MHz), 3dB pad, LPF2 (83 MHz)
- "X Wide": HPF2 (18.2 MHz), 3 dB pad, LPF option (86 MHz).

Thus, all of the LPF and HPF filters of Table 1 are included.

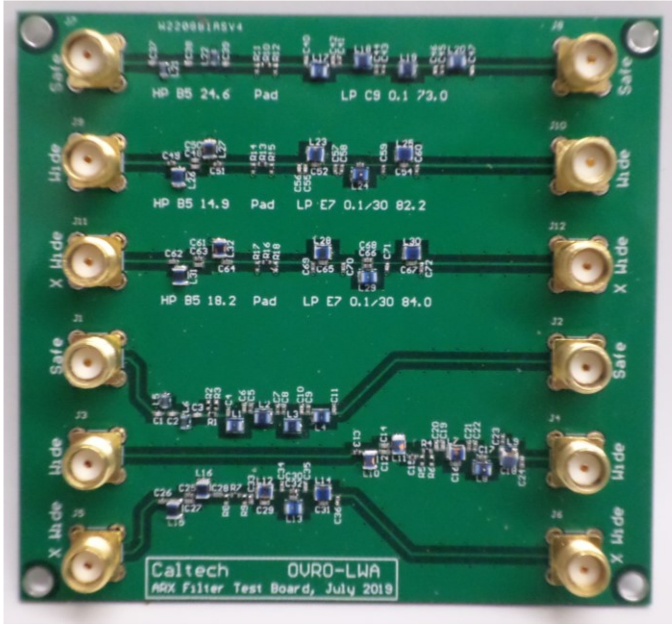

Figure 9. Photo of the filter test board. There are three different bandpass filters constructed as cascades of the HPF and LPF filters in Table 1 using the components in Table 2. Each filter is implemented twice, first using a loose layout (top) and then a tight layout (bottom)..

The S parameters of each filter were measured from 0 to 200 MHz with 0.1 MHz resolution using a Keysight Field Fox vector network analyzer. Results are plotted in Figs. 10-12. The transfer functions from the simulations of both the ideal and practical filters are plotted with the measurements of |S21|.

There is very good agreement between the simulations and the measurements. In all cases the measured band-center insertion loss is equal to or better than the simulated value. For the low-frequency (highpass) filters, all three measure transfer functions lie between the ideal and practical simulations. As expected, the most difficult implementations are the sharp-cutoff elliptical lowpass filters, which have closely-spaced poles and zeros at the band edge (Figs. 9-10). The deep resonances of the two zeros at the stopband edge are not seen in the practical filters (simulated and real) because the inductors have finite Q, but the frequencies seem to be accurate. The third zero near 130-140 MHz is accurately achieved. The design value minimum stopband attenuation, –30 dB, is accurately achieved and occurs at the intended frequency. The passband resonances seen in the |S22| measurements (simulations not done) are close to what is expected for the ideal filters.

Differences between the tight-layout and loose-layout filters appear to be mostly attributable to the 1% and 2% component tolerances rather than to affects of the layouts. An exception might be the "X Wide" filter (Fig. 12), where the passband resonances of the elliptical lowpass seen in |S22| are several MHz lower for the tight layout.

VII. Analysis and Discussion

The test board results (Section VI) show that all the filters can be implemented in practice so that the performance is a good match to the simulations. Even sharp-cutoff elliptical filters can be approximated well. The calculated effect of the filters on the measured spectrum of one signal (Section V) seems to show that even the widest-bandwidth filtering ("LPF option" and "HPF option") provides sufficient RFI suppression. We expect to be able to set the signal levels to the digitizers low enough to tolerate total RFI power at least 10 dB above the desired signal power and still high enough that quantization noise on the desired signal is negligible [6].

However, some caution is needed before adopting the widest bandwidth filtering. First, whereas inductors and capacitors with better than 1% tolerance are not readily available we must

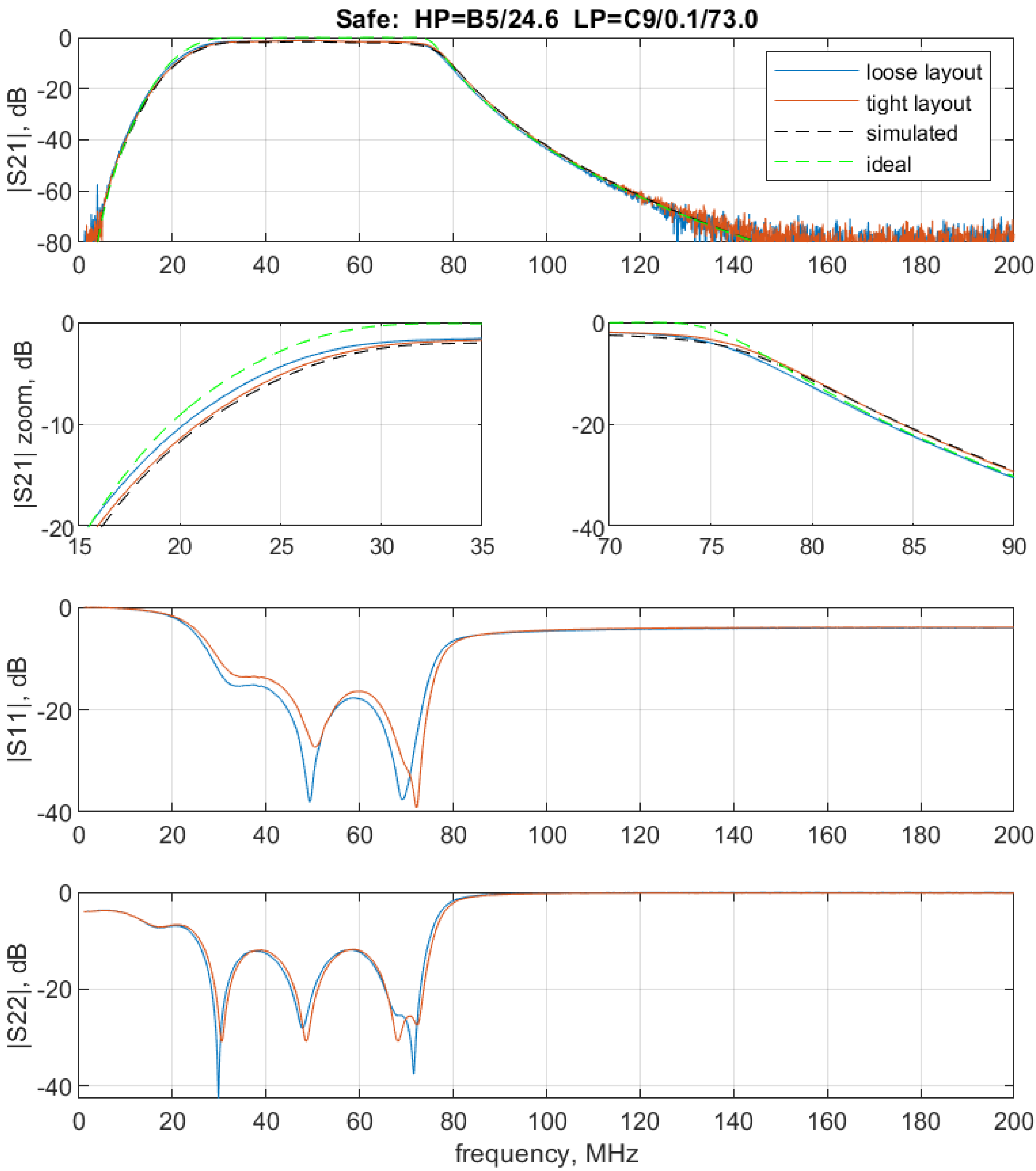

Figure 10. Measurements of the HPF1-LFP1 ("Safe") filter, approximately 25 to 76 MHz at –3 dB. The top plot is the transfer function, showing the measured results for the loose layout (blue) and the tight layout (red) along with the simulated results for actual (dashed black) and ideal (dashed green) components (same as Fig. 4). The plots of the measurements have 2 dB added to compensate for the 2d B attenuator on the test board. The second row shows the same results in expanded views of the lower- and upper-cuttoff regions. The 3rd and 4th rows show the input (HPF side) and output (LPF side) reflection coefficients, respectively.

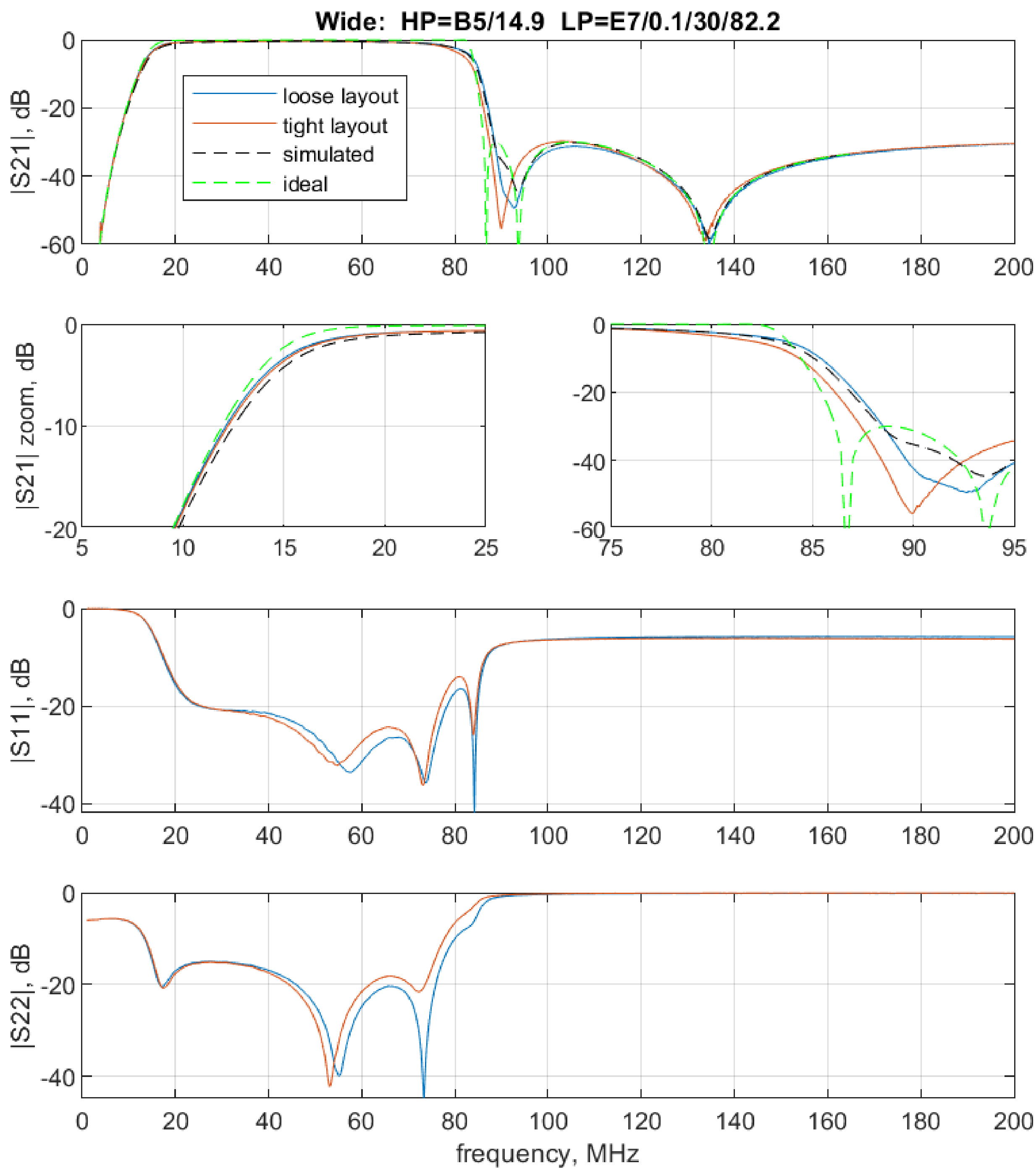

Figure 11. Measurements of the HPFoption-LFP2 ("Wide") filter. This achieves sharper high-frequency cutoff using an elliptical, enabling the upper 3 dB frequency to be increased to about 83 MHz. The low-frequency –3 dB point is decreased substantially to about 15 MHz using the optional LPF. The |S21| measurements have 3 dB added to compensate for the 3 dB attenuator on the test board. Arrangement of the information is the same as in Figure 8.

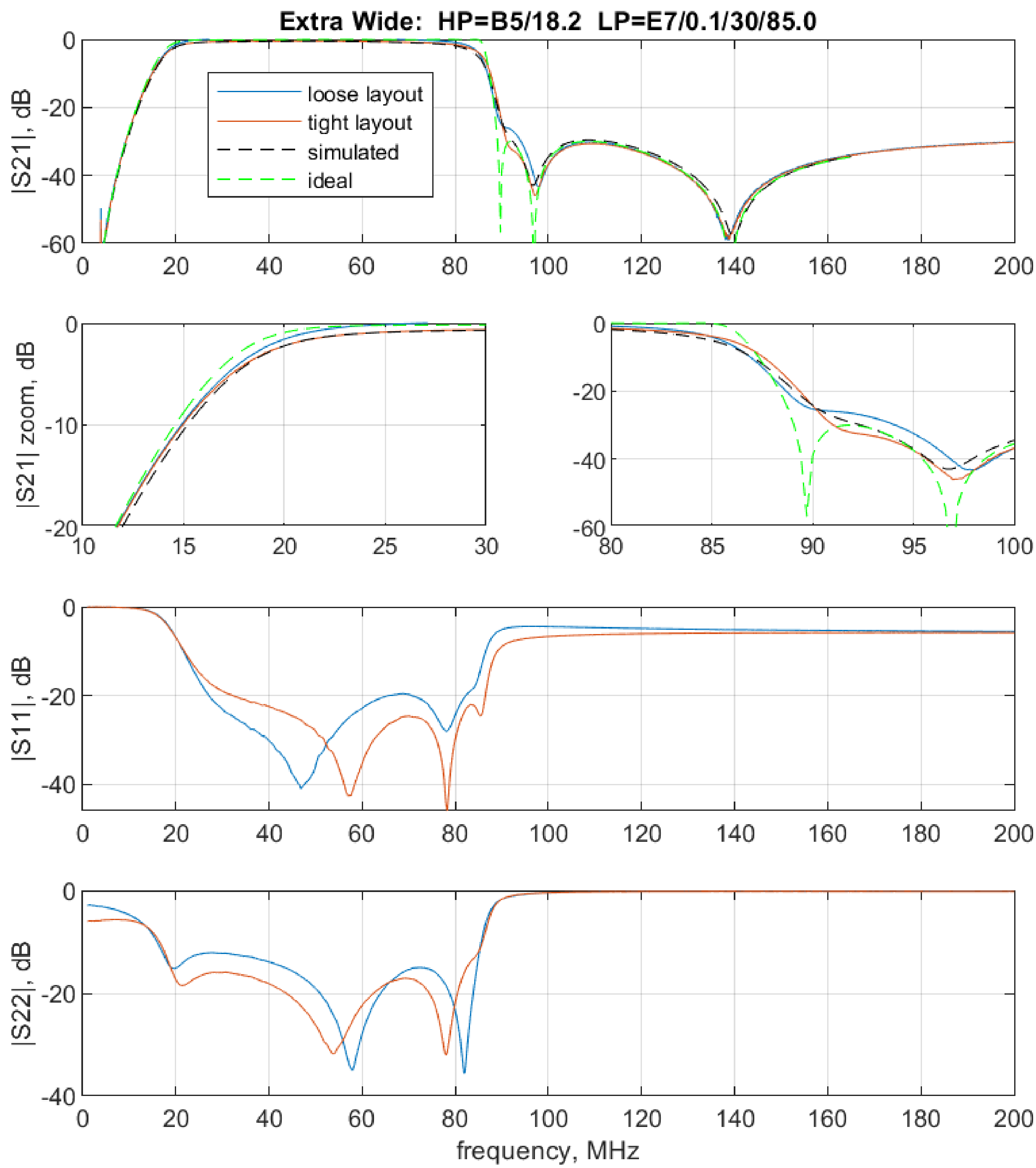

Figure 12. Measurements of the HPF2-LFP option ("X Wide") filter. This pushes the high-frequency –3 dB point to about 86 MHz. The low-frequency –3 dB point is at about 18 MHz, in between the other two cases. The |S21| measurements have 3 dB added. Arrangement of the information in the plots is the same as in Figure 8.

anticipate some variation in performance across a production run of size 800 (704 signals in LWA352, plus spares). The transfer function zeros near 100 MHz are likely to be several MHz away from the design values on some units. Therefore, the FM radio suppression of the aggressive "LPF option" filter (typically 85 MHz at –3 dB) will be sometimes be worse than is seen in Fig. 8.

Second, the typical RFI environment may be different from that observed for one signal on one date (depicted in Fig. 3 and Fig. 7). The low-frequency RFI is highly time-variable, so a much longer data set is needed to understand its statistics. The high-frequency RFI for signal 160B is dominated by a single FM radio station, but antenna 160 is on the south edge of the array, directly exposed to that station's transmitter in Independence, but somewhat shielded by the other antennas from FM radio transmitters to the North, such as in Bishop. Data are needed from other antennas.

It would be surprising if the worst low-frequency RFI exceeds the peak shown in Fig. 7, where it is 25 dB above the observing band power. Fig. 3 shows that the power in that peak is mostly below 10 MHz, so it is well suppressed by the filters. Even with the "HPF option" filter, the peak RFI should be low enough to be accommodated within the dynamic range of the ADCs. From Fig. 8, it seems that filter "HPF1" is more conservative than will ever be needed. Therefore, we choose to use "HPF2" and "HPF option" in the new ARX design.

For the high-frequency RFI, all of the filters, including both their simulations and their implementations on the test board, provide sufficient suppression of the RFI observed from signal 160B. For the elliptical-design filters, the cutoff is so sharp that a few MHz change of cutoff frequency will have a big effect on the RFI suppression if we place the cutoff too close to the 88 MHz edge of the RFI band. To mitigate the risk that the RFI spectrum may be different in the future and different for different antennas, we choose to keep the Chebyshev filter, "LPF1". Its –3 dB frequency of about 76 MHz should allow observing to at least 80 MHz. Its monotonic attenuation increase in the stopband makes it relatively insensitive to unit-to-unit variations from component tolerances. The "LPF option" filter has a nominal –0.1 dB point of 85 MHz, which is very close to the RFI band edge; this makes it sensitive to component tolerances. The "LPF2" option has this at 82.2 MHz, which may be too conservative. Therefore, we select for the new ARX design the "LPF1" filter and a 5th order elliptical like "LPF2" but with cutoff between the two filters tested here, 83.7 MHz at –0.1 dB.

These choices are still subject to refinement based on further measurements of actual RFI in the array (longer duration measurements of low-frequency RFI and measurements using more antennas for high-frequency RFI), and based on further measurements of the filter test board. For example, the test board can be modified to change the cutoff frequency of the elliptical filters.

References

[1] G. Hallinan and co-PIs, "Key Science Projects and Technical Requirements." OVRO-LWA memo, work in progress; latest version 2019 June 07.

[2] OVRO LWA TAC, "LWA Expansion: Technical Advisory Committee Report." Results of the Preliminary Design Review, 2019 June 17-18.

[3] L. D'Addario and N. Marwaha, "Proposed Filters For Next-Generation Analog Receivers." OVRO LWA Memo, 2019 May 2.

[4] B. Hicks, S. Burns, T. Clarke, *et al.*, "Design of the LWA-1 Array, Antenna, Stand, Front End Electronics, and Ground Screen." LWA internal report, 2009 May 15. (A preliminary version is published as LWA Memo 188, 2009 Feb 20.)

[5] L. D'Addario and M. Hodges, "RFI Environment at the OVRO LWA: Quantitative Measurements." OVRO LWA Memo, 2019 April 20.

[6] L. D'Addario, "Effective Dynamic Range of Digitizers in the OVRO-LWA Telescope/" OVRO LWA Memo, 2019 April 27.

ARX Filter Selection

Larry R. D'Addario
California Institute of Technology
2019 July 15

I. Introduction

The next-generation analog receivers being developed for OVRO-LWA352 will have three selectable bandpass filters. The preliminary designs for these filters are described in [1] and were presented at the Preliminary Design Review of 2019 June 17. The designs have progressed to selection of specific, available components and detailed simulations of performance, taking into account non-ideal behavior of practical inductors and parasitic effects of PC board layout. However, the performance has not yet been verified by fabrication and testing.

This memo summarizes the expected performance and attempts to respond to a suggestion in the PDR report of the Technical Advisory Committee (TAC) that frequency coverage be extended to lower frequencies than had previously been considered.

The filter designs attempt to maximize the useful frequency range while suppressing out-of-band RFI. The worst RFI is from the 88-108 MHz FM radio band, and all filters have an average attenuation across that band of at least 20 dB. The "Wide" filter uses an elliptical-response lowpass to obtain sharp cutoff. The "Safe" filter is less sharp but has montonicaly increasing attenuation in the stopband. The "Smooth" filter is still less sharp but nominally has no ripple and less group-delay variation in the passband. At the low end of the band, there is a similar variation in sharpness of response, so the cutoff frequencies vary in order to obtain similar supression of RFI below 20 MHz.

All three filters provide a useful response down to 20 MHz, even though the lowest required frequency among the science cases [1] is 25 MHz. Nevertheless, the TAC recommended [2] that we "consider changes to the filters in order to enable additional science at the low end of the band when conditions are good. Such a change should be properly motivated by documented scientific justification." No suggestion for a new lower limit was given, nor was it stated which of the baseline filters should be replaced, nor what features should be sacrificed.

II. Data

The –3 dB cutoff frequencies (relative to the 50 MHz insertion loss) of the baseline filters are given in Table 1, and the responses are shown in more detail in Figure 1. The "practical"

Table 1: Baseline Filter Designs

	Lower -3dB Freq., MHz			Upper -3dB Freq., MHz		
	Wide	Safe	Smooth	Wide	Safe	Smooth
Ideal (design)	17.5	22.9	22.0	86.1	80.1	75.0
Practical (simulated)	19.3	24.3	23.8	84.4	78.2	71.0

filters include parasitic resistances and reactances of specific COTS components, primarily the inductors. In all cases, the practical filters have less bandwidth (higher low-end cutoff and lower high-end cutoff) than the ideal filters. During the final design process, it may be possible to make small changes that will bring the practical responses closer to the ideal ones.

Figure 2 (from [5]) shows the 24h dynamic spectrum of a signal from a core antenna. No filtering was applied after the front end electronics (which includes only a 150 MHz LPF and slow roll-off below 10 MHz due to d.c. blocking capacitors). This shows that the RFI below 20

MHz is highly time-variable, so it can be expected that there are some periods of low RFI at some frequencies. The Wide filter provides only a few dB of suppression of the 15-20 MHz range, and it is likely that some of the time this will cause intermodulation in the amplifiers of the Analog Receivers (ARXs) or signal clipping in the analog-to-digital converters, especially when combined with the stronger FM-band RFI. Both the Safe and Smooth filters provide considerably more suppression in this range.

Figure 3 (reproduced from [5]) shows that the LWA antennas are expected to have little sensitivity below 20 MHz. The radiation resistance and mismatch efficiency are nearly zero. In spite of the $f^{-2.55}$ frequency dependence of sky noise, the signal is not sky-noise-dominated; at 15 MHz it is about 75% receiver noise.

III. Discussion

Even though the antenna sensitivity is much reduced below 20 MHz, the fact that we see substantial RFI (Fig.2) implies that it has some sensitivity to signals from the sky (perhaps a few percent of that of an antenna tuned to that range). The actual sensitivity is somewhat uncertain because Fig. 3 is based on imperfect simulations, not field measurements.

We could certainly provide a filter with lower cutoff frequency. It would even be possible to use a low-pass filter that provides essentially no attenuation down to about 5 MHz, where roll-off from blocking capacitors becomes significant. Time-domain flagging of RFI might then yield significant intervals with scientifically useful measurements. If the filter provides sufficient suppression of the FM-radio RFI, attenuators in the ARX could be set to prevent intermodulation or clipping, allowing observations to continue at higher frequencies even during substantial RFI, but perhaps at reduced sensitivity compared with what could be obtained with one of the baseline filters. Alternatively, the attenuators could be set to

It is impractical to provide more than three selectable filters, so it is necessary to decide which of the baseline filters to replace.

The filter choices are made difficult by the intension that this telescope will mostly be used commensally, with multiple science programs processing the same signals. There will thus be one filter that is used most of the time and that must provide sufficient suppression of both low-end and high-end RFI to avoid intermodulation and clipping while still providing as much useful bandwidth as possible.

The three baseline filters are *not* intended to support different kinds of observing; rather, they are intended to mitigate the risk that we will not choose the commensal-observing filter correctly. There is some uncertaintly about the RFI environment, and there is uncertainty about how much intermodulation and clipping are tolerable, especially for mid-band observations of maximum sensitivity. The Safe filter is reasonably expected to provide sufficient RFI immunity, but it is possible that the Wide filter will also be sufficient, in which case we will be able to support certain high-frequency and low-frequency science at the same time as sensitive mid-band science. At the high end, both of these filters (but especially the Wide filter) provide sharp cutoff, and this necessarily produces rapidly-varying phase response and group delay (see Figure 4). It is uncertain that this phase part of the gain can be adequately calibrated; the Smooth filter is provided to mitigate that risk.

Unfortunately we will not have enough field experience to remove these uncertainties until long after the full telescope is deployed, and we do not have funding to replace all the filters (effectively all the ARXs) at that time.

If this design philosophy of risk mitigation were abandoned, so that we select in advance a single filter design for the commensal observing, then we could design the remaining two filters to provide extended low-frequency bandwidth and high-frequency bandwidth, respectively. The latter filters would then be used primarily for specialized observations. In that case, the commensal-observing filter would need to have a rather conservative design, perhaps like the Smooth filter (Butterworth prototype) but with even less bandwidth for more RFI rejection.

IV. Conclusion

The engineering team needs guidance from the science team on the filter selections. How strong is the scientific case for *any* coverage below 20 MHz, considering the low antenna sensitivity? How strong is the scientific case for *commensal* coverage above 70 MHz? How important is it to have a *smooth* gain-vs.-frequency function (in phase as well as amplitude), considering the difficulties of accurate astronomical bandpass calibration?

References

[1] G. Hallinan and co-PIs, "Key Science Projects and Technical Requirements." OVRO-LWA memo, work in progress; latest version 2019 June 07.

[2] OVRO LWA TAC, "LWA Expansion: Technical Advisory Committee Report." Results of the Preliminary Design Review, 2019 June 17-18.

[3] L. D'Addario and N. Marwaha, "Proposed Filters For Next-Generation Analog Receivers." OVRO LWA Memo, 2019 May 2.

[4] B. Hicks, S. Burns, T. Clarke, *et al.*, "Design of the LWA-1 Array, Antenna, Stand, Front End Electronics, and Ground Screen." LWA internal report, 2009 May 15. (A preliminary version is published as LWA Memo 188, 2009 Feb 20.)

[5] L. D'Addario and M. Hodges, "RFI Environment at the OVRO LWA: Quantitative Measurements." OVRO LWA Memo, 2019 April 20.

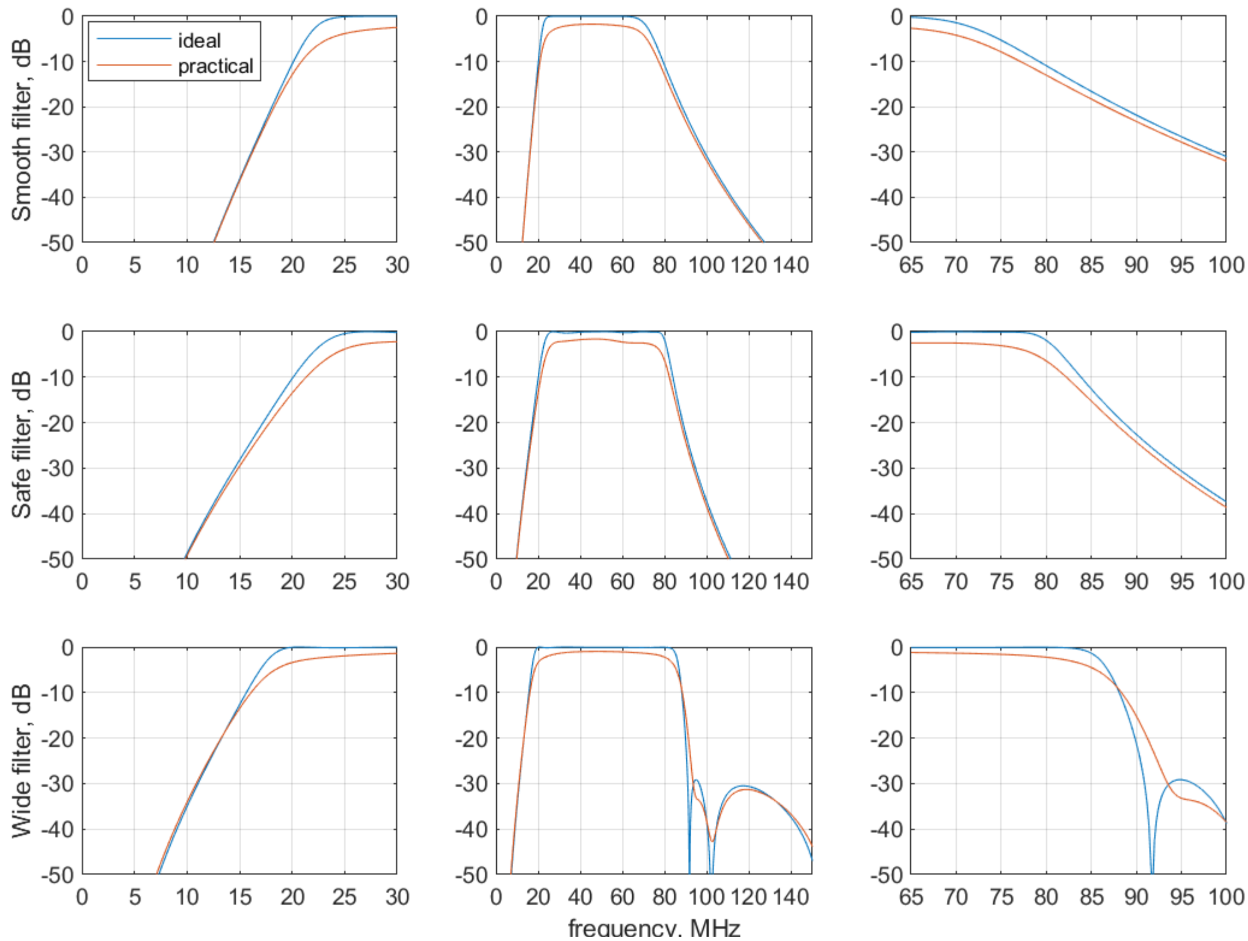

Figure 1. Simulated responses of the three filters of the preliminary design, with expanded views of the lower and upper cutoff regions. In each case, the ideal response and the practical response (with available capacitors and inductors, including detailed modeling of inductor parasitics) are given.

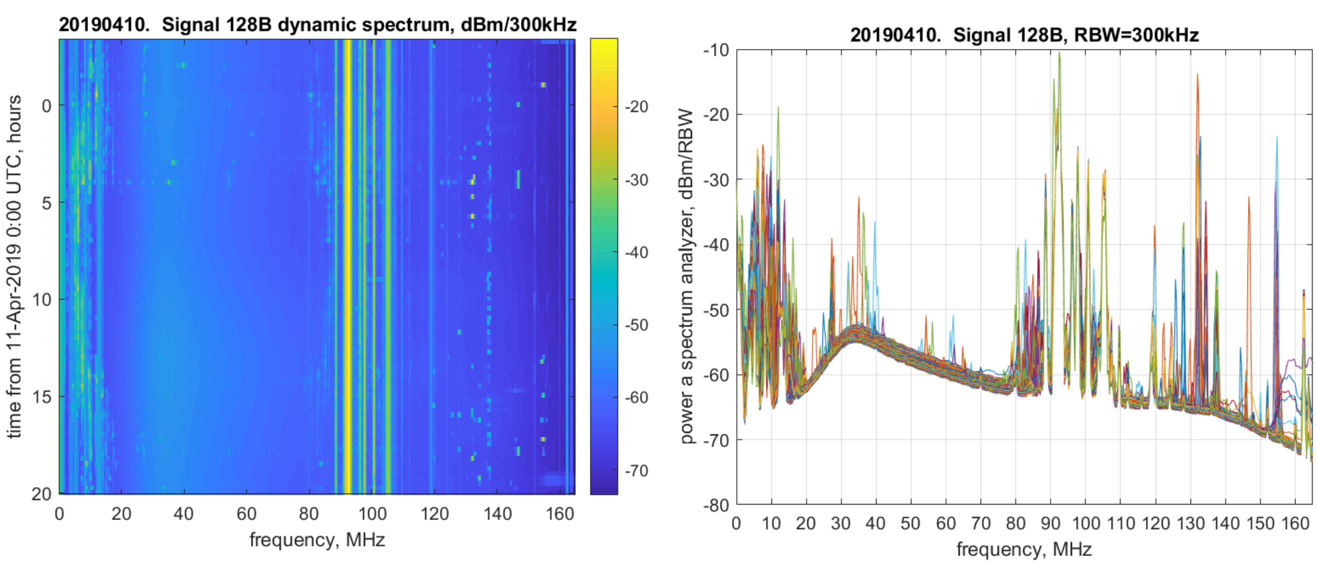

Figure 2. Dynamic spectrum of a signal from a core antenna with short coax length (every 15m for 24h), along with all spectra overlayed. No filtering, but a 28dB broad-band amplifier preceded an Agilent spectrum analyzer. From [5]; see that report for details of the setup..

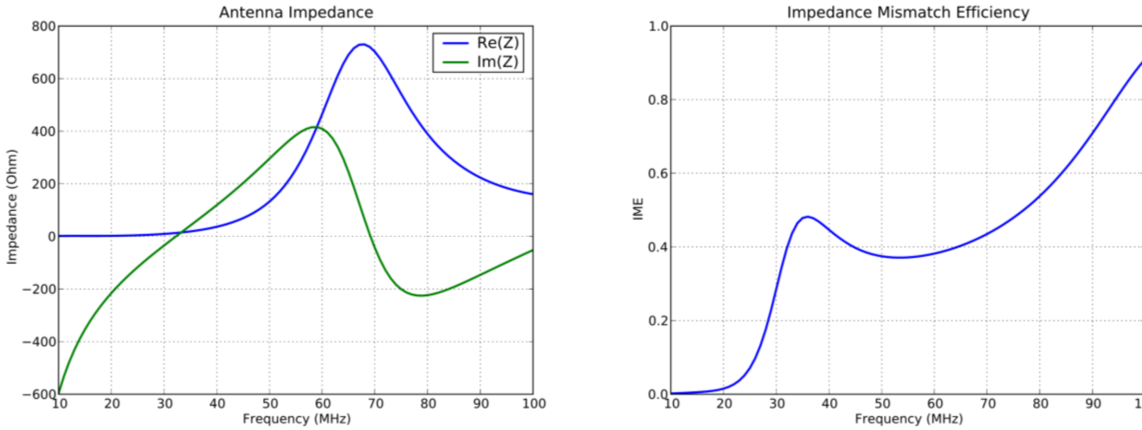

Figure 2.5: Antenna terminal impedance and impedance mismatch efficiency

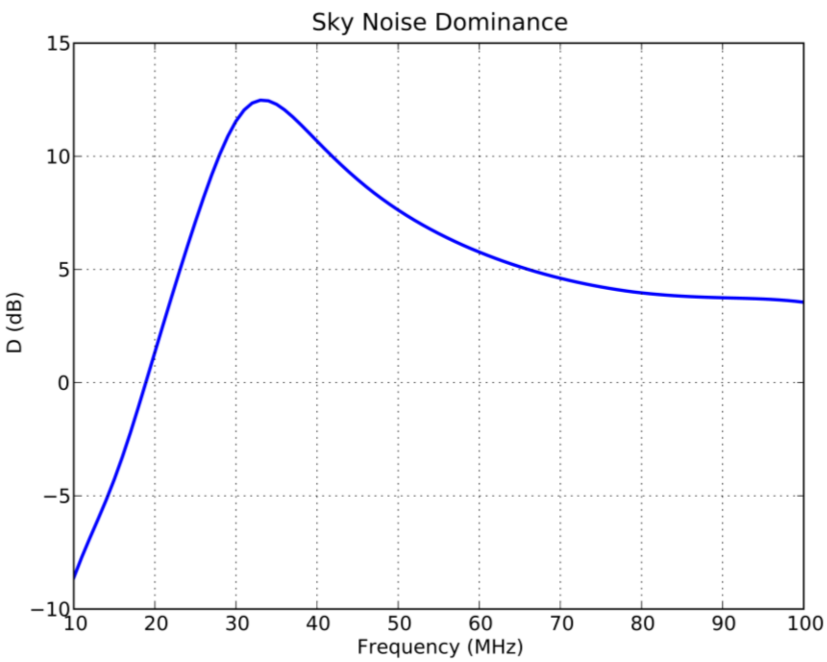

Figure 2.6: Predicted sky noise dominance (D) for ANT + GND as a function of frequency including impedance mismatch and ground losses calculated using NEC-4 and assuming T_{FEE} = 250 K and Z_{FEE} = 100 Ω. The Cane [16] model for sky noise at the Galactic pole is assumed, so this is a minimum sky noise dominance.

Figure 3. LWA antenna terminal impedance, mismatch efficiency, and sky noise dominance (system temperature/receiver temperature), from [4].

I

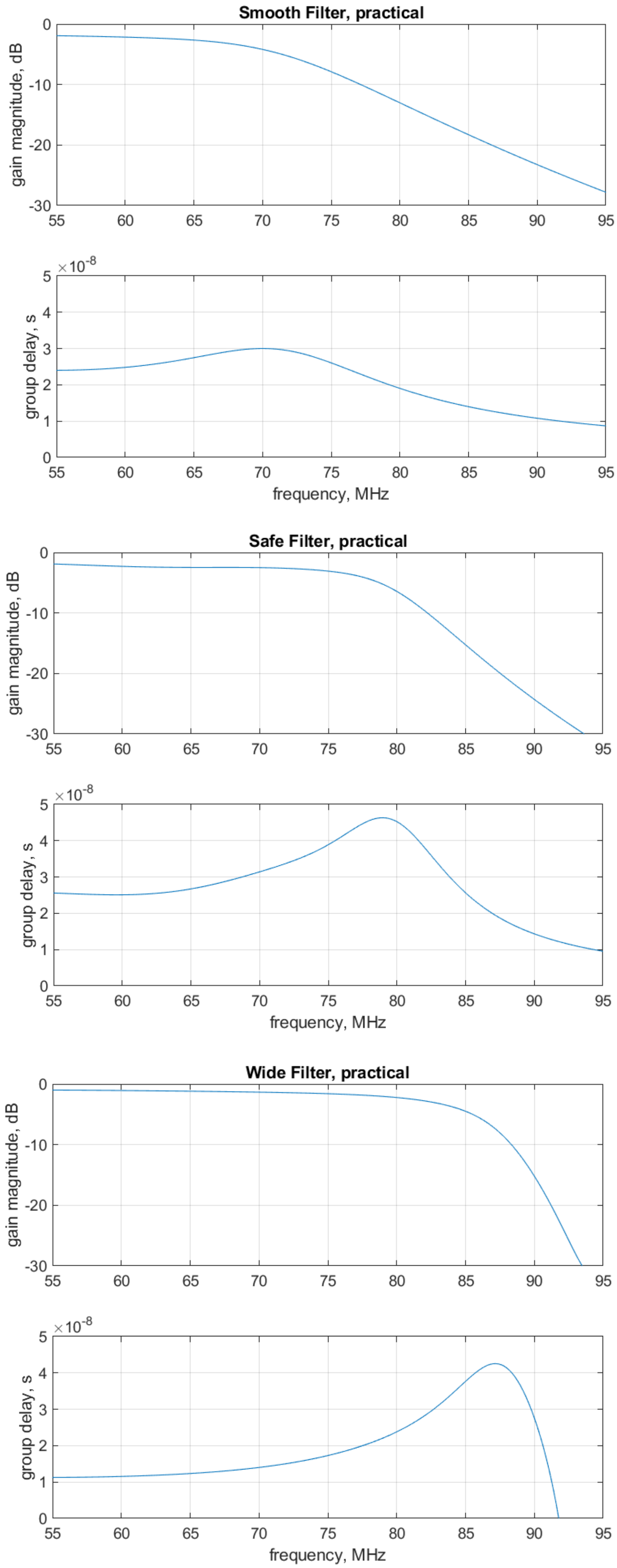

Figure 4. Responses of the three baseline-design filters near their upper cutoff frequencies, including the group delays. As the sharpness of cutoff increases, the group delay variation is larger.

Proposed Filters For Next-Generation Analog Receivers

Larry R. D'Addario and Nitika Marwaha
California Institute of Technology
2 May 2019 (original version: 15 April 2019)

Abstract— It is proposed to provide three selectable filters in the new analog receivers, and to call them the "wide", "safe", and "smooth" filters. The first provides the widest possible bandwidth while suppressing out-of-band RFI just enough that intermodulation caused by digitizer clipping with 8-bit digitizers is avoided most of the time, provided that the signal level to each digitizer is correctly set. The second assures that digitizer clipping is almost always avoided, while providing some margin for non-optimum signal levels. Both of these use filters that create small ripples in the passband, and they produce delays that vary rapidly near the band edges. The third filter is smoother, with no passband ripple and less delay variation, but has smaller usable bandwidth. The theoretical –3 dB points of the filters are, respectively, (17.5,86.1), (22.9,80.1), and (22.0,72.5) MHz. These preliminary choices are based on the performance that could be obtained with ideal components of exactly the optimum values; simulations in LTSpice show that adequate performance can be achieved with practical ones in commercially-available values.

I. Introduction

It was shown earlier [1] that if the signal level is carefully set, then 8-bit digitizers allow broadband RFI to have a total power 20.7 dB above that of the diurnal-maximum 25-85 MHz ("in band") total power without significant intermodulation. In recent tests [2], it was found that at the LWA antenna's front end output the peak total power over 24h in the <20 MHz and >88 MHz bands are, respectively, 17 dB above and 26 dB above the peak in-band total power (neglecting transient in-band RFI); see Figure 1. The low-side RFI level is highly variable (and usually <10 dB above the in-band power) while the high-side RFI is quite stable. From this it appears that the low-side RFI can be tolerated without further filtering (relying on digital filtering and flagging post-digitization), while the high-side RFI must be suppressed by at least

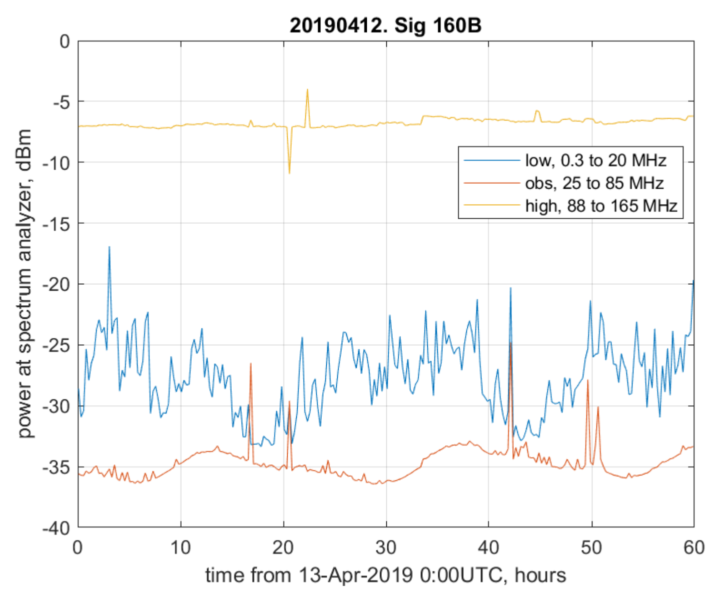

Figure 1. Example of results from 60h of observations of an LWA antenna signal, from [2]. Each curve is the total power integrated over the given bandwidth. A spectrum was measured every 15 minutes.

26 dB – 20.7 dB = 5.3 dB prior to digitization. However, we choose to be conservative by providing filtering that suppresses out-of-band signals by at least 10 dB more than these results suggest.

II. Ideal Responses of the Proposed Filters

Three switchable filters are proposed. Their theoretical transmission functions, for ideal components, are plotted in Figure 2. For the >88 MHz band, which needs the most suppression, the safe and smooth filters have –20 dB transmission at 88 MHz, but with different steepness of cutoff. To achieve the very steep cutoff of the "wide" filter, it has equal-amplitude ripple in the stop band with peaks at –30 dB; it reaches –30 dB at 90.8 MHz and has –10.4 dB transmission at 88 MHz. The others have monotonically increasing attenuation with frequency. For the <20 MHz band, the "smooth" and "safe" filters have –10 dB transmission at 20 MHz but the "wide" filter reaches –10 dB at 15 MHz. Perhaps surprisingly, the smooth filter achieves slightly steeper cutoff than the safe filter; this is a result of its structure, discussed below.

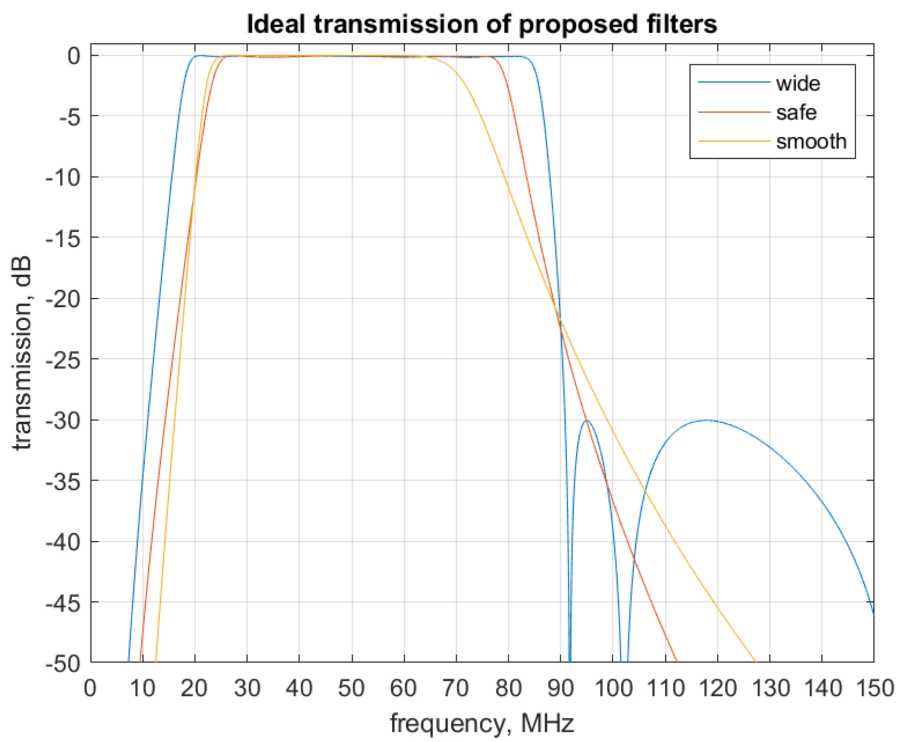

Figure 2: Filter responses with ideal components.

Some properties of the filters are given in Table 1. The average transmission in the lower RFI band and in the FM radio band (which dominates the upper RFI band) are given, along with the 3 dB points. For all filters, we seem to have considerable margin over the suppression required, but it is not guaranteed because the RFI is not uniformly distributed in frequency.

Table 1

Filter	*Avg. transmission over 2-20 MHz*	*Avg. transmission over 88-108 MHz*	*Lower –3 dB frequency*	*Upper –3 dB frequency*
Wide	–23.4 dB	–24.2 dB	17.5 MHz	86.1 MHz
Safe	–27.3 dB	–27.8 dB	22.9 MHz	80.1 MHz
Smooth	–26.0 dB	–26.3 dB	22.0 MHz	75.0 MHz

III. Implementations

The responses of Fig. 2 can be achieved with the following structures.

- Wide: cascade of
  - HPF Chebyshev I, order 5, –0.1 dB min. passband from 20.0 MHz;
  - LPF Elliptical, order 7, –0.01 dB min. in passband to 82.2 MHz, –30 dB max. in stopband.
- Safe: cascade of
  - HPF Chebyshev I, order 5, –0.1 dB min. passband from 26.0 MHz;
  - LPF Chebyshev I, order 9, –0.1 dB min. passband to 77.0 MHz/
- Smooth: single bandpass filter
  - BPF Butterworth, order 7, –3 dB points at 22.0 MHz and 72.5 MHz.

Schematics of all filters, with optimum component values, are shown in Figure 3-5. They were calculated using [3].

IV. Discussion

These designs are preliminary and the filter parameters are subject to revision. The performances shown are calculated for ideal components and are not likely to be realized in practice. This is especially true for the "wide" filter's sharp high-frequency cutoff.

Only the amplitude responses are plotted in Fig.2. The "wide" and "safe" filters have a phase response that changes rapidly near the cutoff frequencies, leading to variation in group delay across the passband. For interferometry, the delay variations cancel on each baseline if all signal paths are identical, but fabrication tolerances prevent all the filters from being exactly the same. This is expected to lead to a need for delay calibration and correction that varies with frequency.

The feasibility of practical implementations of these filters was explored by simulations in LTSpice. Results of the simulations are summarized in Appendix A. For each filter, 4 versions were simulated:

1. Ideal components with the exact values for the desired response, as in Figs. 3-5. This produces the same responses as Fig. 2.
2. Ideal components but with commercially-available values in 1% or 2% tolerance. Whereas steps between available inductor values are usually larger than between available capacitor values, inductors were chosen first and capacitors were chosen to compensate, where possible. Specific manufacturers and part numbers were carefully selected, as shown in Appendix A.
3. Inductors replaced by realistic models provided by their manufacturer, including parasitic resistances and reactances.
4. Capacitors added to simulate each PCB pad of the surface-mount Ls and Cs, assuming standard pad dimensions for 0402, 0603, and 0805 size devices and a ground place .0081 inch below them with FR4 dielectric.

See Appendix A for details. For most filters, there was little difference between simulations 1 and 2; available components were close enough to the exact values. There was also very little difference between simulations 3 and 4; the pad capacitances are small and have little effect.

The overall result of the simulations is that good performance is predicted for practical implementations. The passband response is rounded near the cutoff frequencies, but the steepness of cutoff and stopband rejection are about right, even for the elliptical lowpass used for the "wide" filter. In all cases, the bandwidths are a few MHz narrower than intended, with the

–6 dB frequencies of the practical filters about the same as the –3 dB frequencies of the ideal ones. If necessary, this can be compensated in another design iteration without changing the topologies.

REFERENCES

[1] L. D'Addario, "Effective Dynamic Range of Digitizers in the OVRO-LWA Telescope." OVRO-LWA internal memo, 2019 March 23.

[2] L. D'Addario, "RFI Environment at the OVRO LWA: Quantitative Measurements." In preparation.

[3] RF Tools, "LC Filters Design Tool." https://rf-tools.com/lc-filter/.

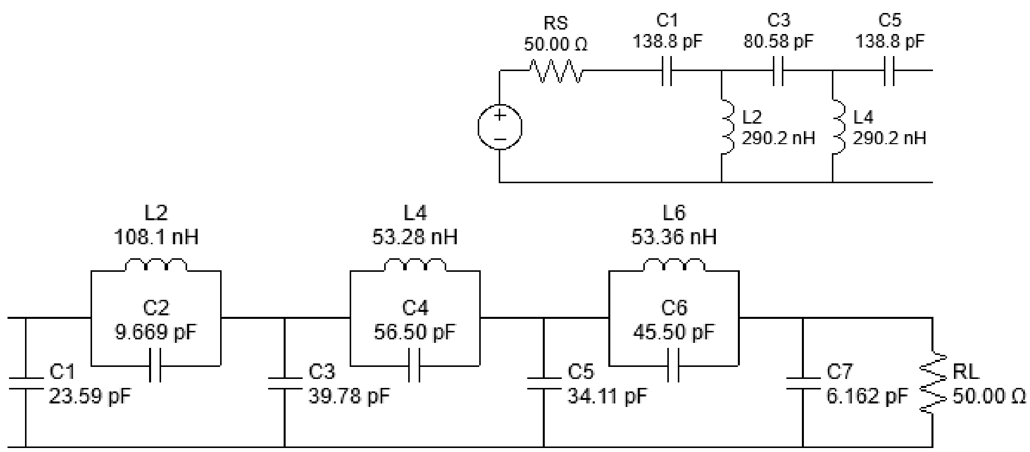

Figure 3. Wide filter implementation.

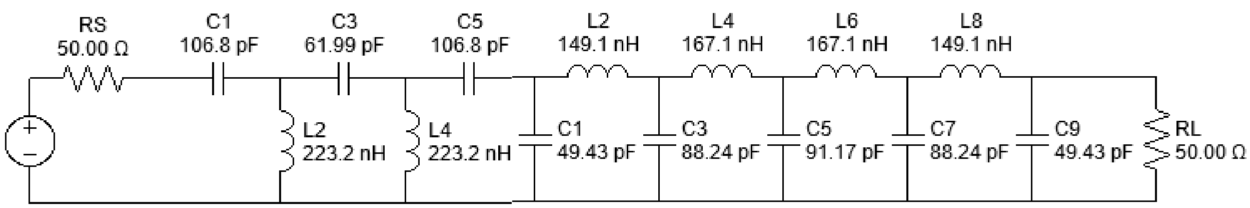

Figure 4. Safe filter implementation.

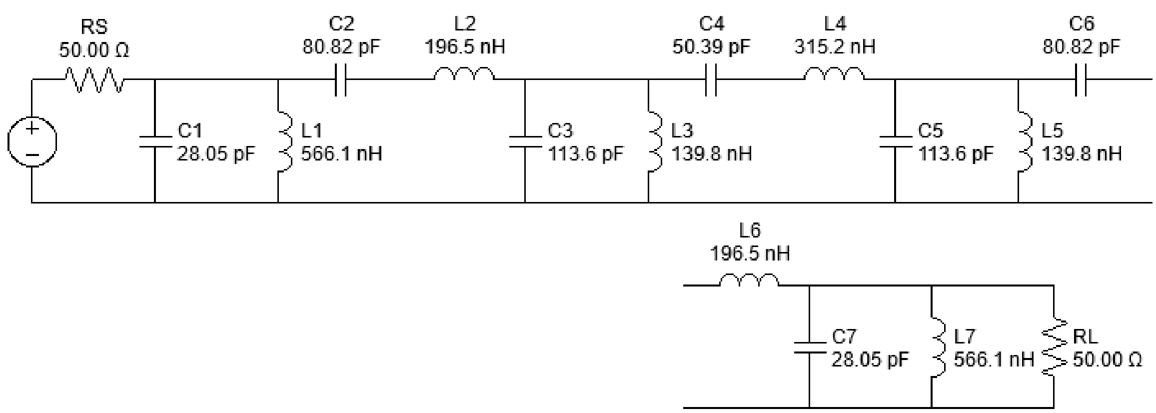

Figure 5. Smooth filter implementation.

Appendix A: LWA-ARX filter simulation summary

I. Wide band filter simulations

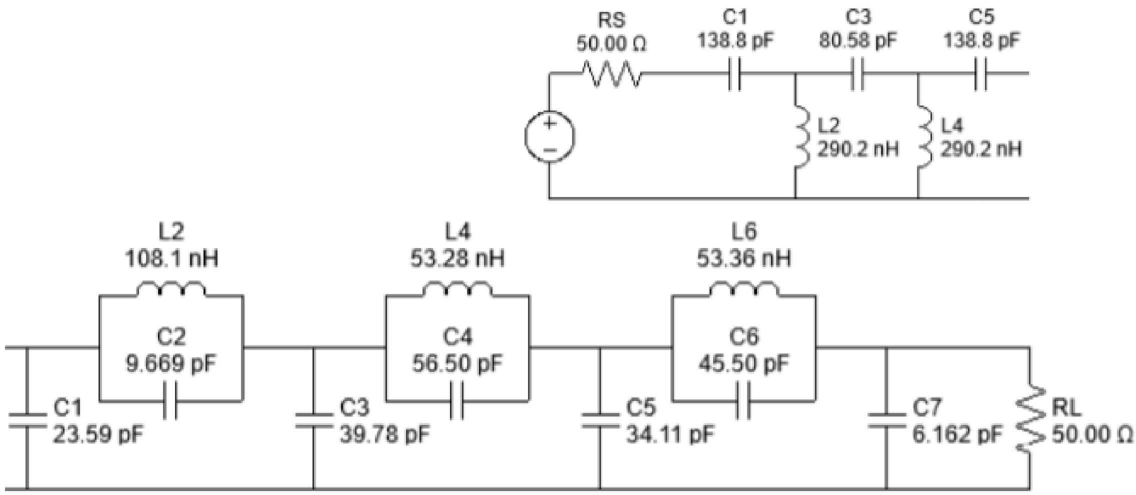

Figure 3. Wide filter implementation.

<u>Inductor selection and the model of the inductor used:</u>

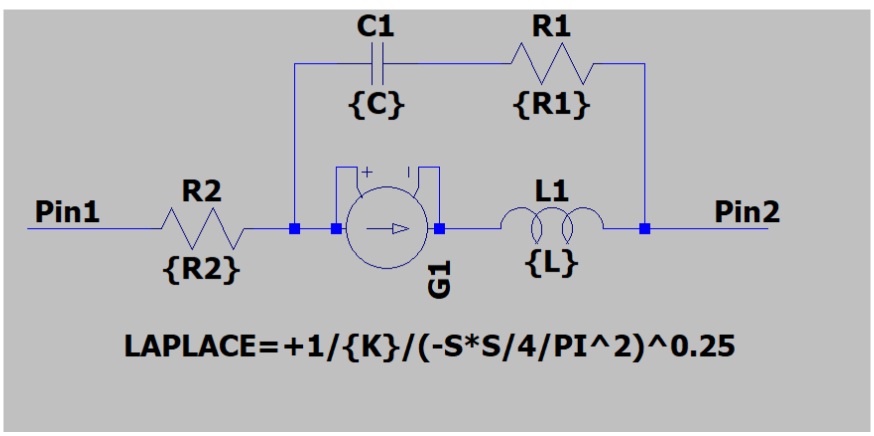

$$R_{VAR} = k * \sqrt{f}$$

- k is shown for each value in the accompanying table.
- f is the frequency in Hz

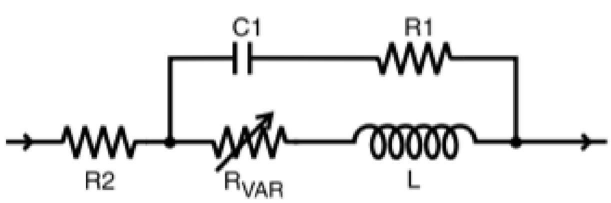

CoilCrafts Inductor families			
0805LS	0805CS	0805AF	0805HP
Lowest DCR	Exceptionally high Q	high current handling	highest Q factor
0.078 µH to 27 µH	2.8 nH to 820 nH	0.11 µH to 22 µH	2.6 nH to 820 nH
−40°C to +85°C	−40°C to +125°C		
Ferrite	Ceramic		Ceramic
Rvar2	No Rvar2	Has Rvar1, Rvar2, Lvar	

0805CS and for some values 0805HP (with 1% or 2% tolerance) inductor family parts are choses for ARX filter design.

LTSpice directive used
.ac dec 100 1Meg 1000Meg

AC voltage of 2V amplitude is chosen to have 0dB loss in the pass band in the ideal condition when Rsource = Rload (Req = 0 ohm)

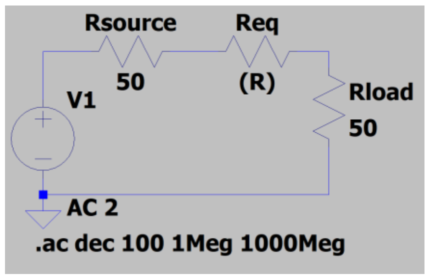

Inductors selected for Wide band filter implementation:

S.No.	Filter exact value (nH)	L @ 50MHz (nH)	Manufacturer	Part number	R1 (ohm)	R2 (ohm)	C (pF)	L (nH)	k	(MHz)	% variation from exact	Nominal Inductance (nH)	L@f (MHhZ)	Tolerance	Q	Q@f (MHz)	DCR max	Irms(mA)	SRF(MHz)	Spice model input	Rtot @50 MHz
1	290.2	270.11	Coilcraft	0805HP-271	15	0.754	0.138	266.1	0.0001454	1000	6.922812	270	100	2,5	27	50	754	200	830	K=0.0001454 C=0.138p R1=15 R2=0.754 L=266.1n	1.78
2	108.1	112.43		0805CS-111	15	0.48	0.109	109	0.000152	1800	-4.00555	110	150	2,5	18	50	480	400	1100	K=0.000152 C=0.109p R1=15 R2=0.48 L=109n	1.55
3	53.28	56.4		0805CS-560	13	0.34	0.094	56	0.000101	2700	-5.855856	56	200	1,2,5	29	50	340	500	1600	K=0.000101 C=0.094p R1=13 R2=0.34 L=56n	1.05
4	53.36	56.4		0805CS-560	13	0.34	0.094	56	0.000101	2700	-5.697151	56	200	1,2,5	29	50	340	500	1600	K=0.000101 C=0.094p R1=13 R2=0.34 L=56n	1.05

- Used 0402 capacitor with 1% tolerance (except for 140pF, which is used in 0805 package)
- Used coilcraft inductors in 0805 CS family, except for 270nH, which is used in 0805HP family, due to lesser ESR and closer inductor value @50MHz

Capacitor selection:

S. No.	Filter exact value (pF)	Value used (pF)	MPN	Manufacturer	Tolerance	Voltage	Temp Coeff	Temp range	Package	Description	Variation
1	138.8	140	08055U141FAT2A	AVX	1	50	C0G, NP0	-55°C ~ 125°C	O804	CAP CER 140PF 50V NP0 0805	-0.864553314
2	80.58	82	GCM1555C1H820FA16D	Murata	1	50	C0G, NP0	-55°C ~ 125°C	O402	CAP CER 82PF 50V C0G/NP0 0402	-1.762223877
3	9.921	10	GJM1555C1H100FB01D	Murata	1	50	C0G, NP0	-55°C ~ 125°C	O402	CAP CER 10PF 50V C0G/NP0 0402	-0.796290697
4	23.59	24	04025U240FAT2A	AVX	1	50	C0G, NP0	-55°C ~ 125°C	O402	CAP CER 24PF 50V NP0 0402	-1.738024587
5	9.669	10	GJM1555C1H100FB01D	Murata	1	50	C0G, NP0	-55°C ~ 125°C	O402	CAP CER 10PF 50V C0G/NP0 0402	-3.423311614
		9.2	GCQ1555C1H9R2BB01D	Murata	0.1pF	50	C0G, NP0	-55°C ~ 125°C	O402	CAP CER 9.2PF 50V C0G/NP0 0402	4.850553315
6	39.78	39	04025A390FAT2A	AVX	1	50	C0G, NP0	-55°C ~ 125°C	O402	CAP CER 39PF 50V C0G/NP0 0402	1.960784314
7	56.5	56	04025A560FAT2A	AVX	1	50	C0G, NP0	-55°C ~ 125°C	O402	CAP CER 56PF 50V C0G/NP0 0402	0.884955752
		51	CBR04C510F5GAC	Kemet	1	50	C0G, NP0	-55°C ~ 125°C	O402	CAP CER RF 51PF 50V 1% C0G 0402	9.734513274
8	34.11	33	GCM1555C1H330FA16D	Murata	1	50	C0G, NP0	-55°C ~ 125°C	O402	CAP CER 33PF 50V C0G/NP0 0402	3.254177661
9	45.5	43	VJ0402D430FXAAJ	Vishay	1	50	C0G, NP0	-55°C ~ 125°C	O402	CAP CER 43PF 50V C0G/NP0 0402	5.494505495
10	6.162	6.2	GJM1555C1H6R2WB01D	Murata	0.05pF	50	C0G, NP0	-55°C ~ 125°C	O402	CAP CER 6.2PF 50V C0G/NP0 0402	-0.616682895

a) HPF part of "wide" filter (n=5 Cheby I, 0.1dB, 20.0 MHz)

- HPF_1: Exact values, ideal components
- HPF_2: available values, ideal components
- HPF_3: available values, specific PN components, full models of inductors
- HPF_4: like HPE_3, but with capacitors added to model PCB pads.

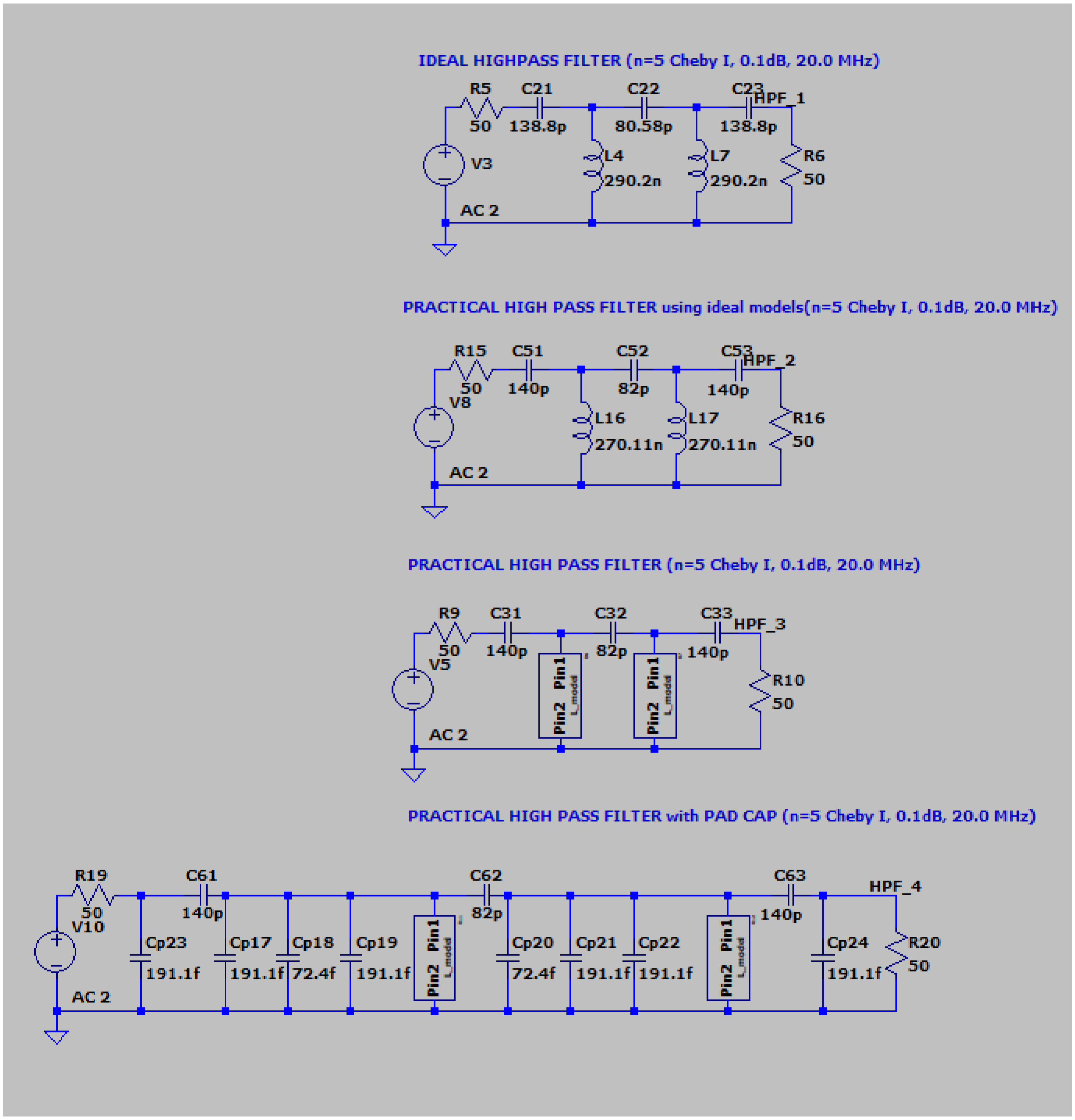

Frequency response for different configurations of High pass filter of the wide band filter response

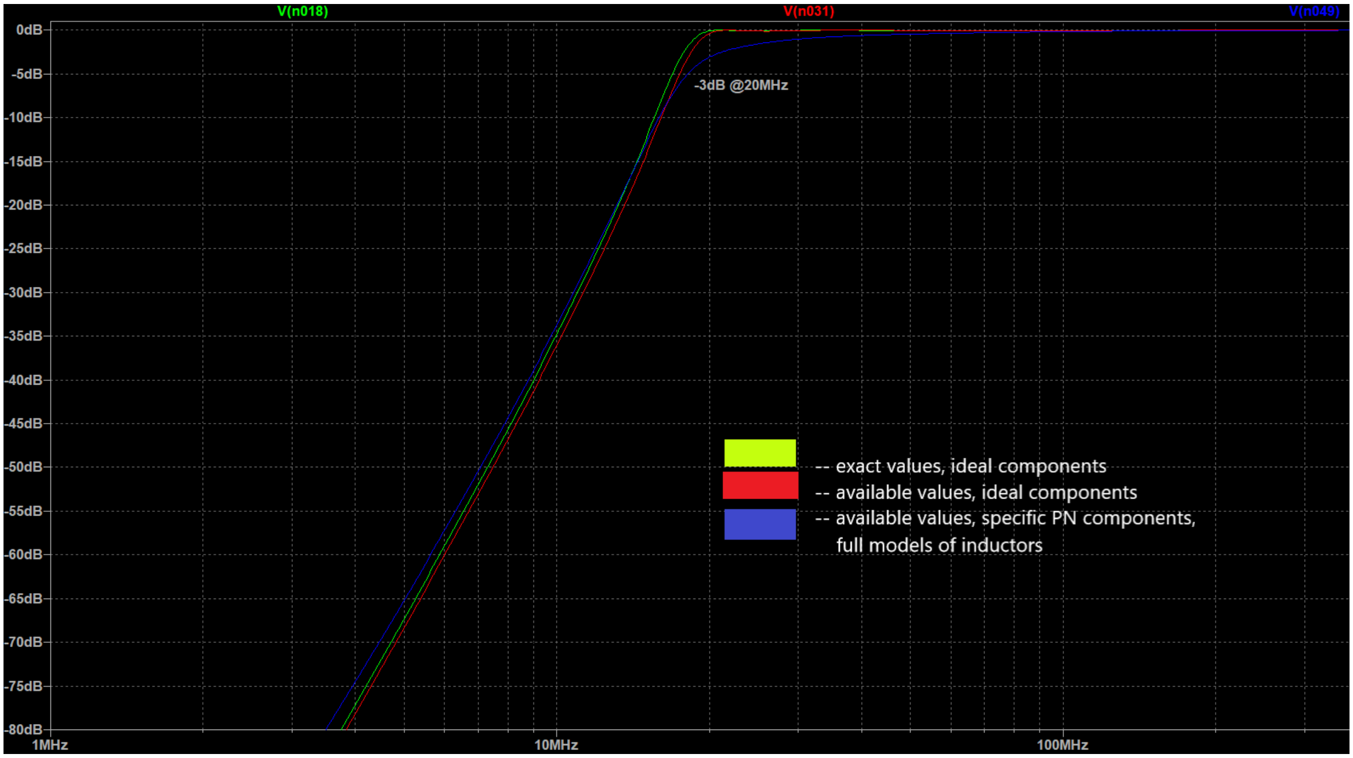

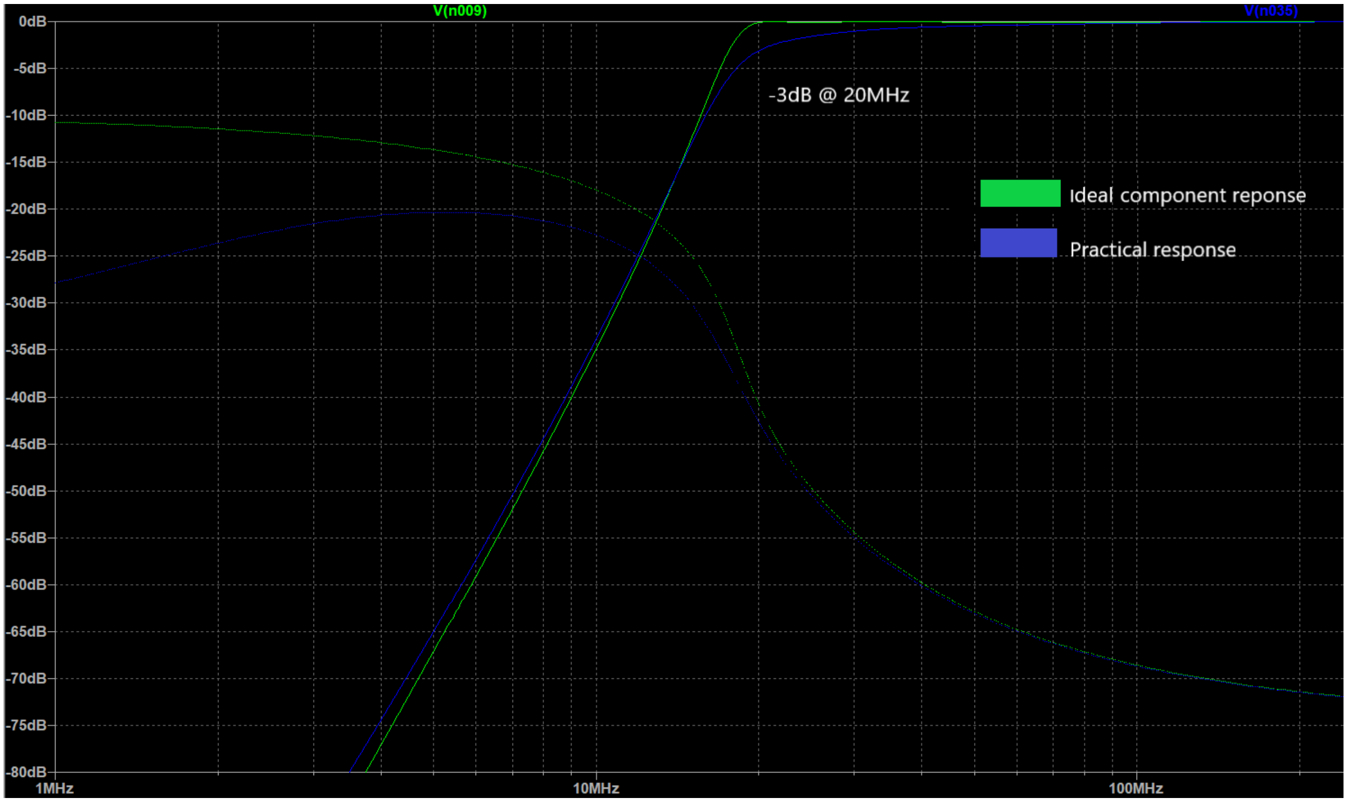

Figure A1: Comparison of HPF_1 and HPF3

- Responses of HPF_1 and HPF_2 are almost identical.
- Responses of HPF_3 and HPF_4 are almost identical.

b) Low pass filter of the wide band filter implementation

- LPF_1: Exact values, ideal components
- LPF_2: available values, ideal components
- LPF_3: available values, specific PN components, full models of inductors
- LPF_4: like LPE_3, but with capacitors added to model PCB pads.

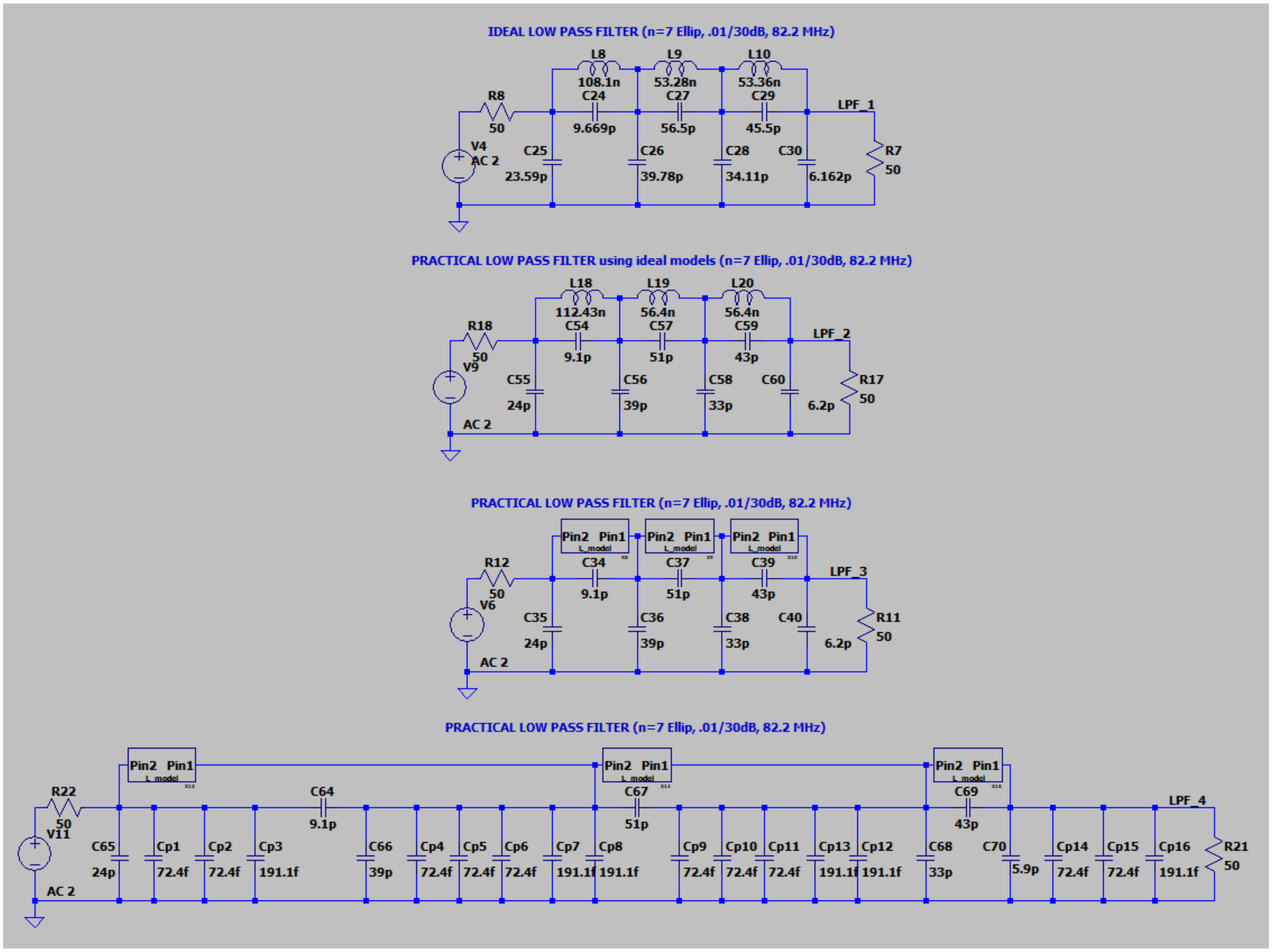

Capacitor value modification based on constant LC resonator frequency

Exact C	Exact L	L variation	C variation	LC variation (should be -1)	Modified C	New available C
9.669	108.1	-4.005550416	-3.42331161	1.170081	9.28170333	9.1
56.5	53.28	-5.855855856	0.884955752	-6.61712	53.19144144	51
45.5	53.36	-5.697151424	5.494505495	-1.03688	42.9077961	43

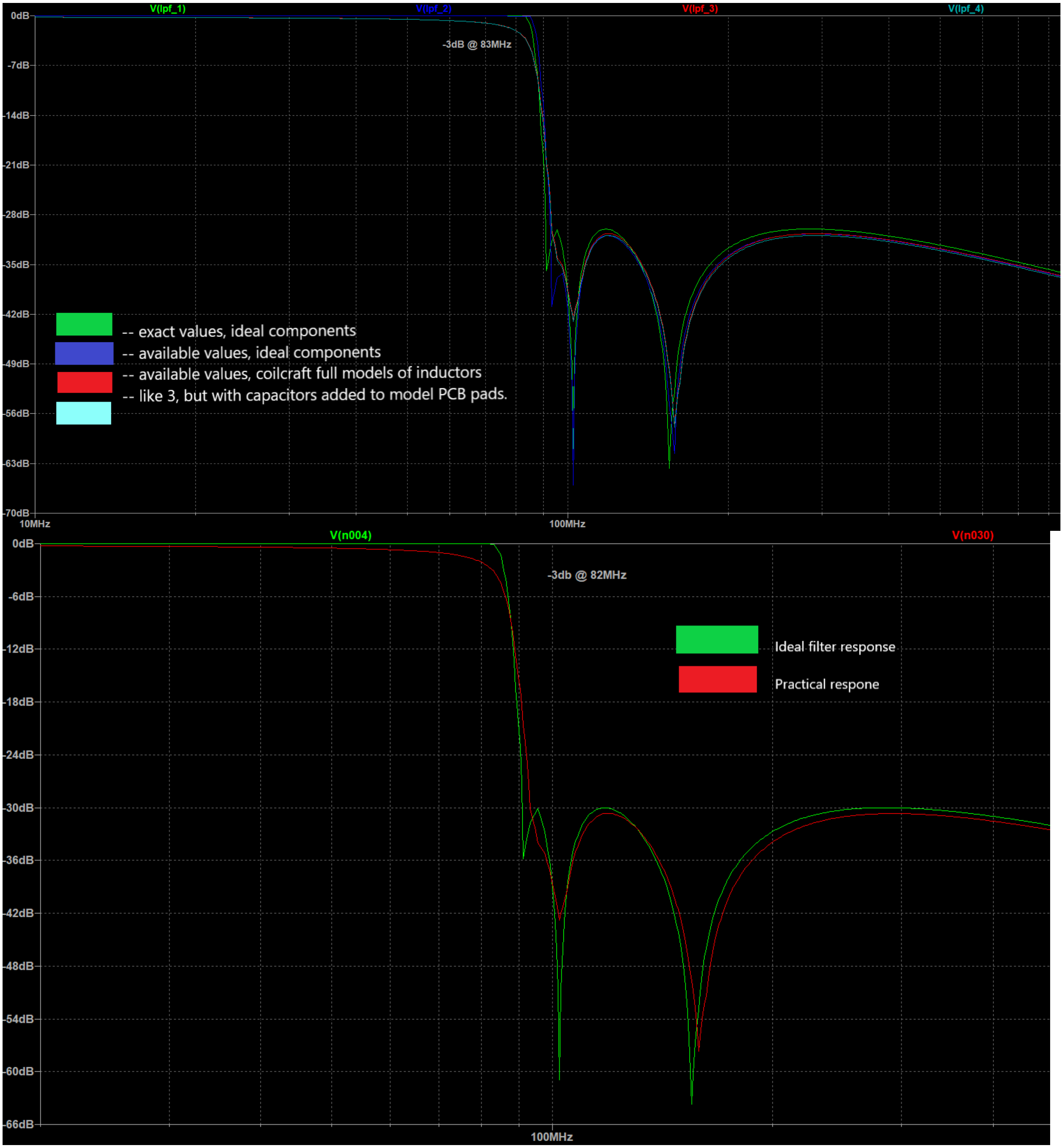

Figure A2: Comparison of LPF_1 and LPF3

- Responses of LPF_1 and LPF_2 are almost identical.
- Responses of LPF_3 and LPF_4 are almost identical.

c) Wide band filter response (Cascaded HPF and LPF)

- BPF_1: Exact values, ideal components
- BPF_2: available values, ideal components
- BPF_3: available values, specific PN components, full models of inductors
- BPF_4: like BPE_3, but with capacitors added to model PCB pads.

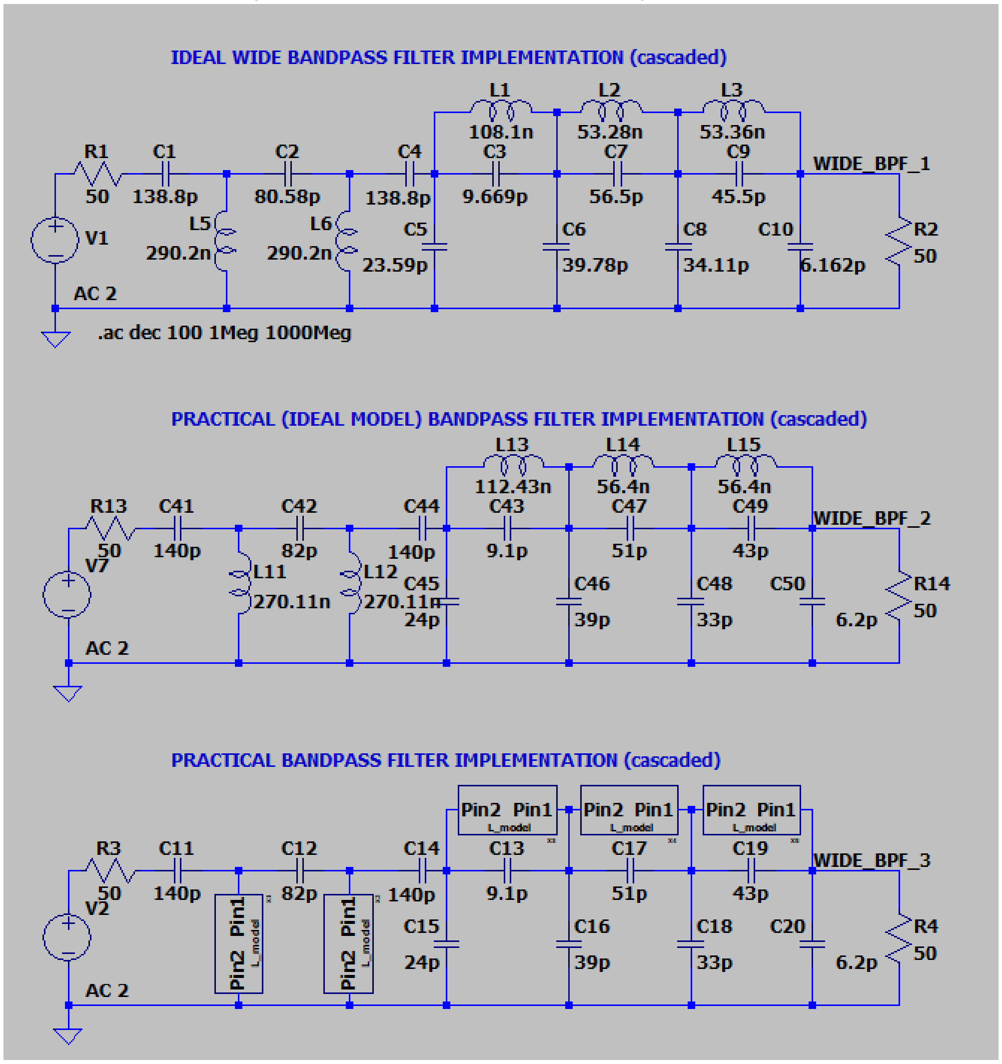

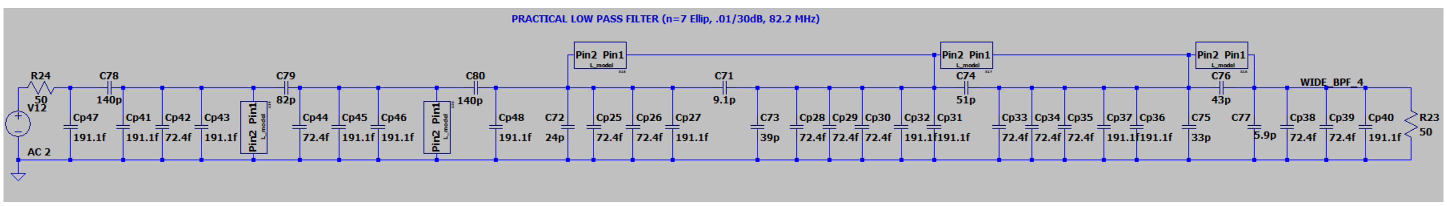

<u>Shunt capacitor modification based on pad-to-ground capacitance</u>

C used(pF)	Cpad_0805(pF)	Cpad_0402(pF)	New C(pF)	Available C(pF)
24	0.1911	0.0724	23.6641	24
39	0.1911	0.0724	38.4006	39
33	0.1911	0.0724	32.4006	33
6.2	0.1911	0.0724	5.8641	5.9

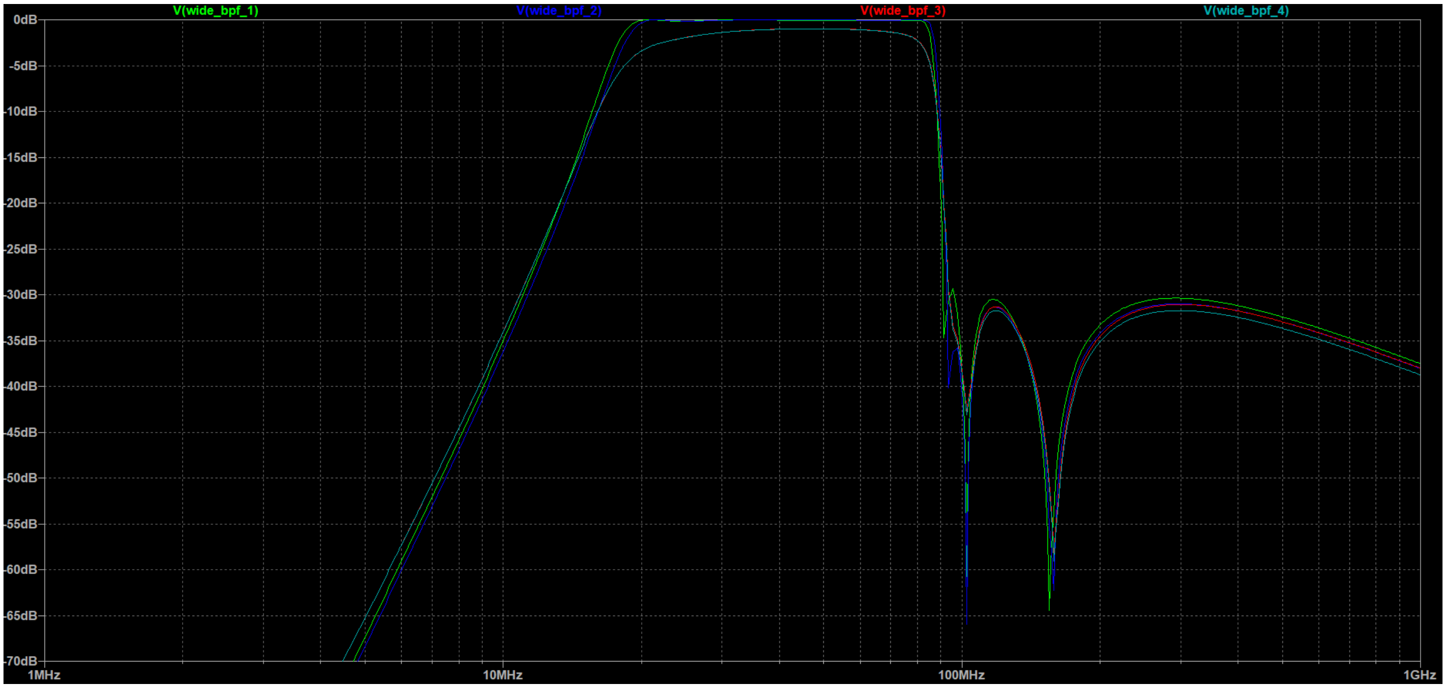

Figure A3: Comparison of BPF_1 and BPF3

- Responses of BPF_1 and BPF_2 are almost identical.
- Responses of BPF_3 and BPF_4 are almost identical.

II. Safe filter simulations

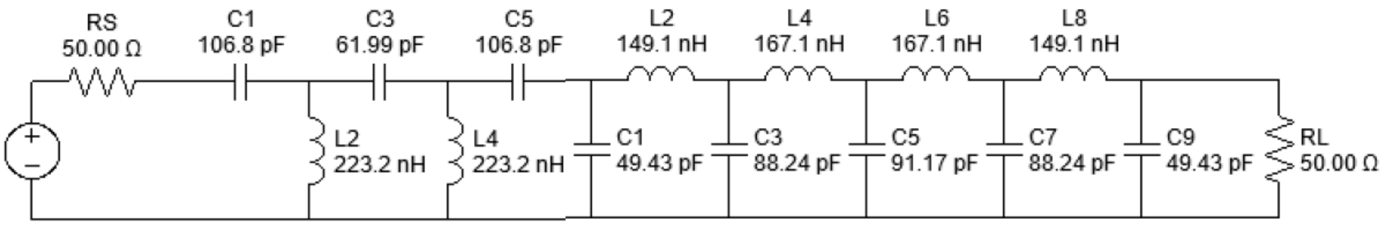

Figure 4. Safe filter implementation.

a) HPF part of "safe" filter (n=5 Cheby I, 0.1dB, 26.0 MHz)

b) LPF part of "safe" filter (n=9 Cheby I, 0.1dB, 77.0 MHz)

<u>Capacitor selection:</u>

S. No.	Filter exact value (pF)	Value used (pF)	MPN	Manufacturer	Tolerance	Voltage	Temp Coeff	Temp range	Package	Description	Variation
1	106.8	110	CC0402JRNPO9BN111	AVX	2	50	NPO	-55°C ~ 12	0402	CAP CER 110PF 50V NPO 0402	-0.864553314
2	61.99	62	04025A620FAT2A	AVX	1	50	C0G, NP0	-55°C ~ 12	0402	CAP CER 62PF 50V NP0 0402	-1.762223877
3	49.43	51	CBR04C510F5GAC	Kemet	1	50	C0G, NP0	-55°C ~ 12	0402	CAP CER RF 51PF 50V 1% C0G 0402	-3.17620878
4	88.24	82	GCM1555C1H820FA16[	Murata	1	50	C0G, NP0	-55°C ~ 12	0402	CAP CER 82PF 50V C0G/NP0 0402	7.071622847
5	91.17	91	06031U910FAT2A	AVX	1	50	NP0	-55°C ~ 12	0603	CAP CER 91PF 100V NP0 0603	0.186464846

- For 88.24pf, using 82pF, as reducing the capacitance made the response closer to the response of idea response.
- Also, using 0603 package for 91pF due to the closed value available in only 0603 pacakge

<u>Inductor selection:</u>

S.No.	Filter exact value (nH)	L @ 50MHz (nH)	Manufacturer	Part number	R1 (ohm)	R2 (ohm)	C (pF)	L (nH)	k	(MHz)	% variation from exact	Nominal Inductance (nH)	L@f (MHhZ)	Tolerance	Q	Q@f (MHz)	DCR max	Irms(mA)	SRF(MHz)	Spice model input	Rtot @50 MHz
1	223.2	220.93	Coilcraft	0805CS-221	26	0.7	0.086	215	3.40E-04	1500	1.01702509	220	100	2,5	34	50	700	400	820	K=0.00034 C=0.086p R1=26 R2=0.7 L=215r	3.1
2	149.1	151.64		0805CS-151	24	0.56	0.11	149	2.23E-04	1500	-1.7035547	150	100	1,2,5	31	50	560	400	1150	K=0.000223 C=0.11p R1=24 R2=0.56 L=149r	2.14
3	167.1	179.42		0805CS-181	18	0.64	0.09	178	2.75E-04	1600	-7.3728306	56	200	1,2,5	29	50	340	500	1600	K=0.000275 C=0.09p R1=18 R2=0.64 L=178i	2.58

- Used coilcraft inductors in 0805 CS family

a) HPF part of "safe" filter (n=5 Cheby I, 0.1dB, 26.0 MHz)

- SAFE_HPF_1: Exact values, ideal components
- SAFE_HPF_2: available values, ideal components
- SAFE_HPF_3: available values, specific PN components, full models of inductors
- SAFE_HPF_4: like HPE_3, but with capacitors added to model PCB pads.

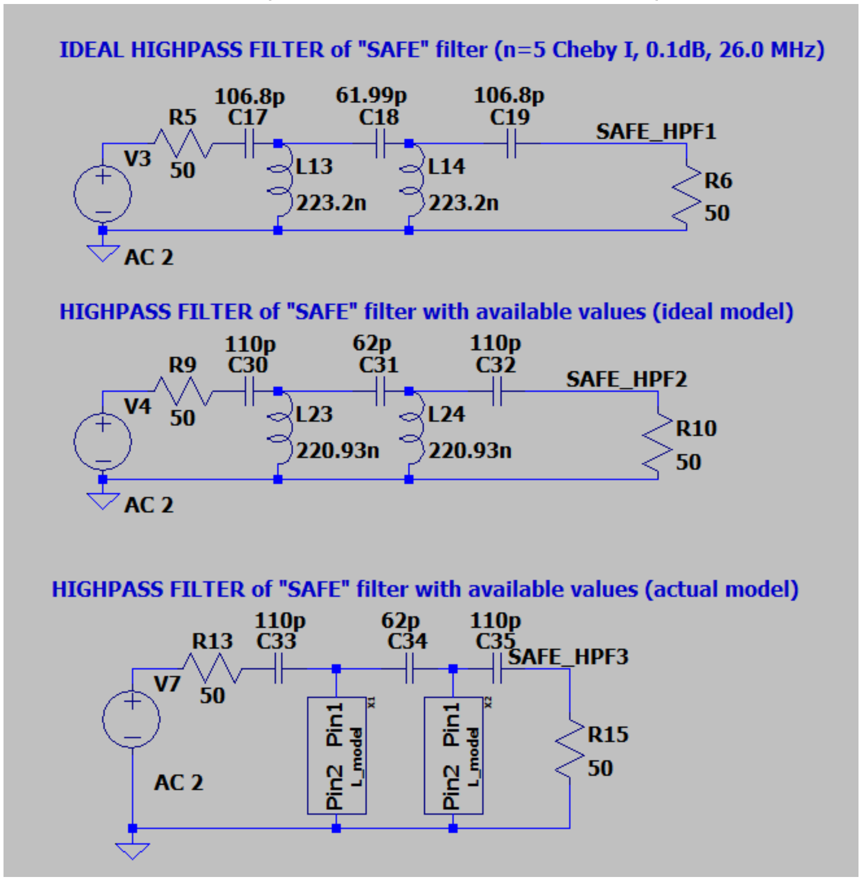

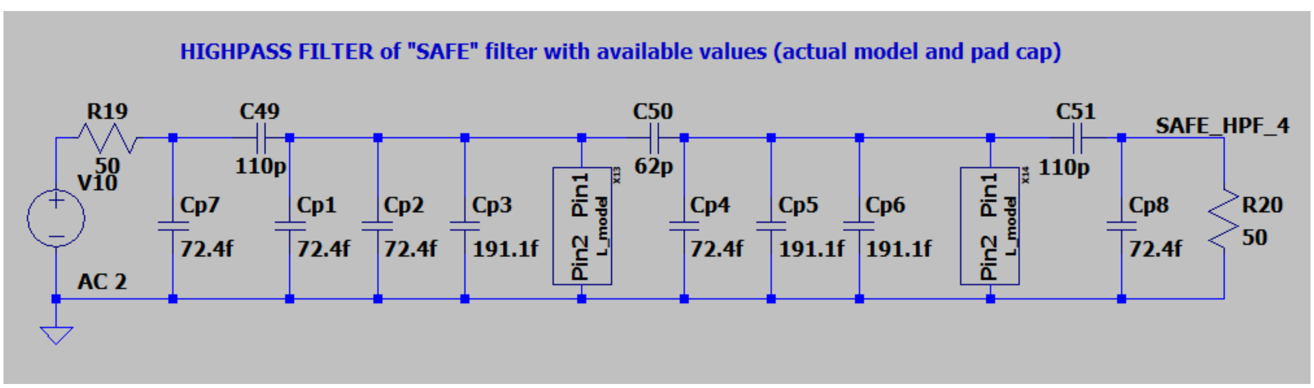

Frequency response for different configurations of High pass filter of the safe band filter response

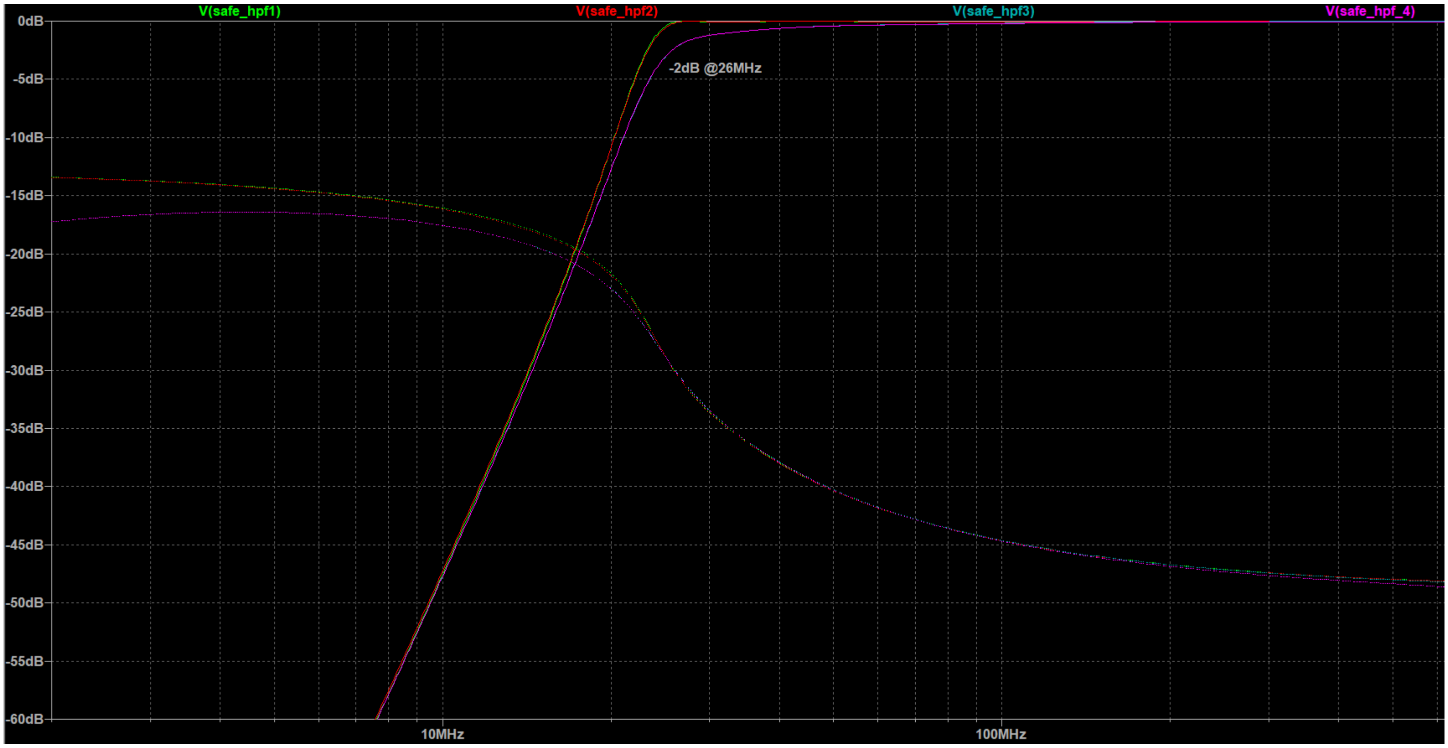

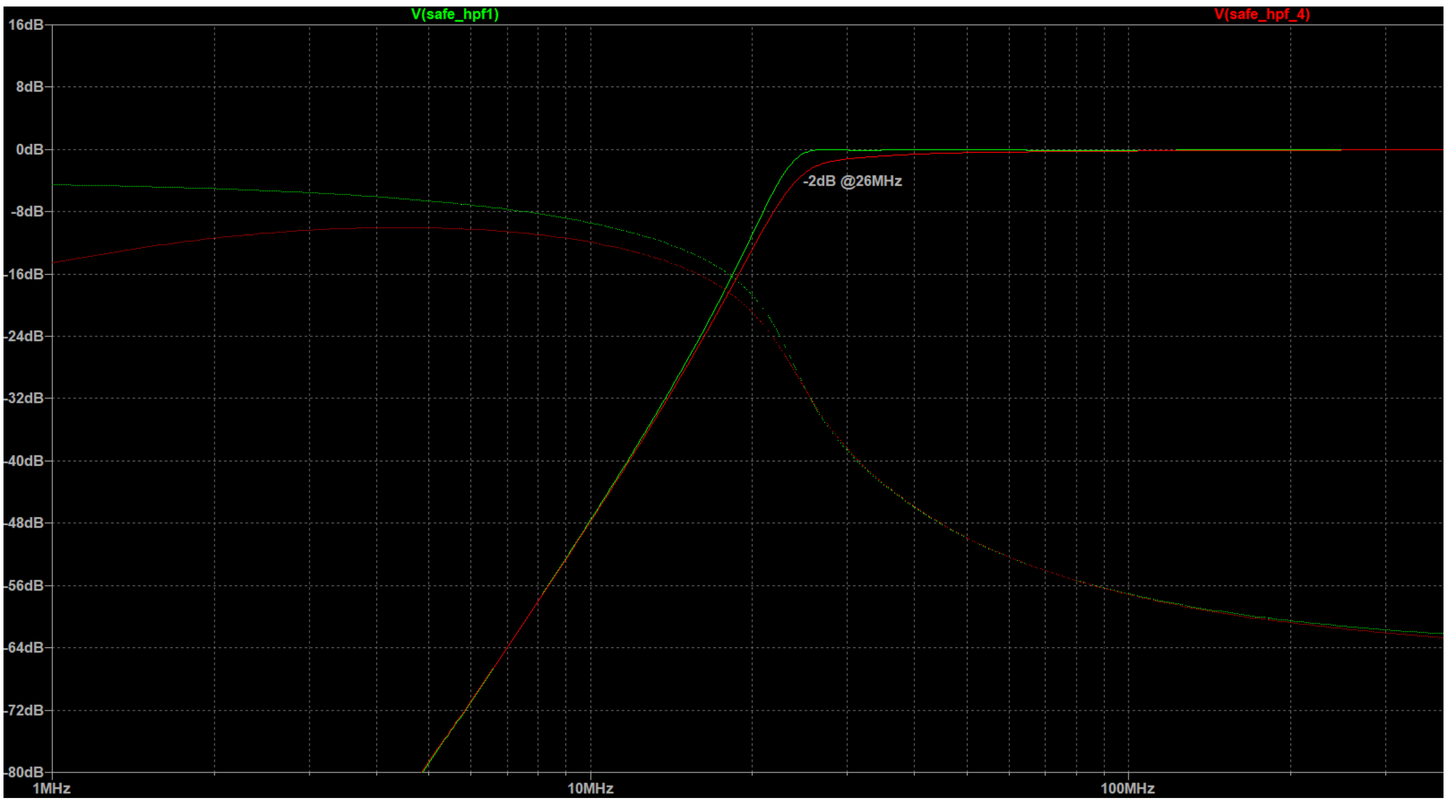

Figure A4: Comparison of SAFE_HPF_1 and SAFE_HPF4

- Responses of SAFE_HPF_1 and SAFE_HPF_2 are almost identical.
- Responses of SAFE_HPF_3 and SAFE_HPF_3 are almost identical.

b) LPF part of "safe" filter (n=9 Cheby I, 0.1dB, 77.0 MHz)

- SAFE_LPF_1: Exact values, ideal components
- SAFE_LPF_2: available values, ideal components
- SAFE_LPF_3: available values, specific PN components, full models of inductors
- SAFE_LPF_4: like LPE_3, but with capacitors added to model PCB pads.

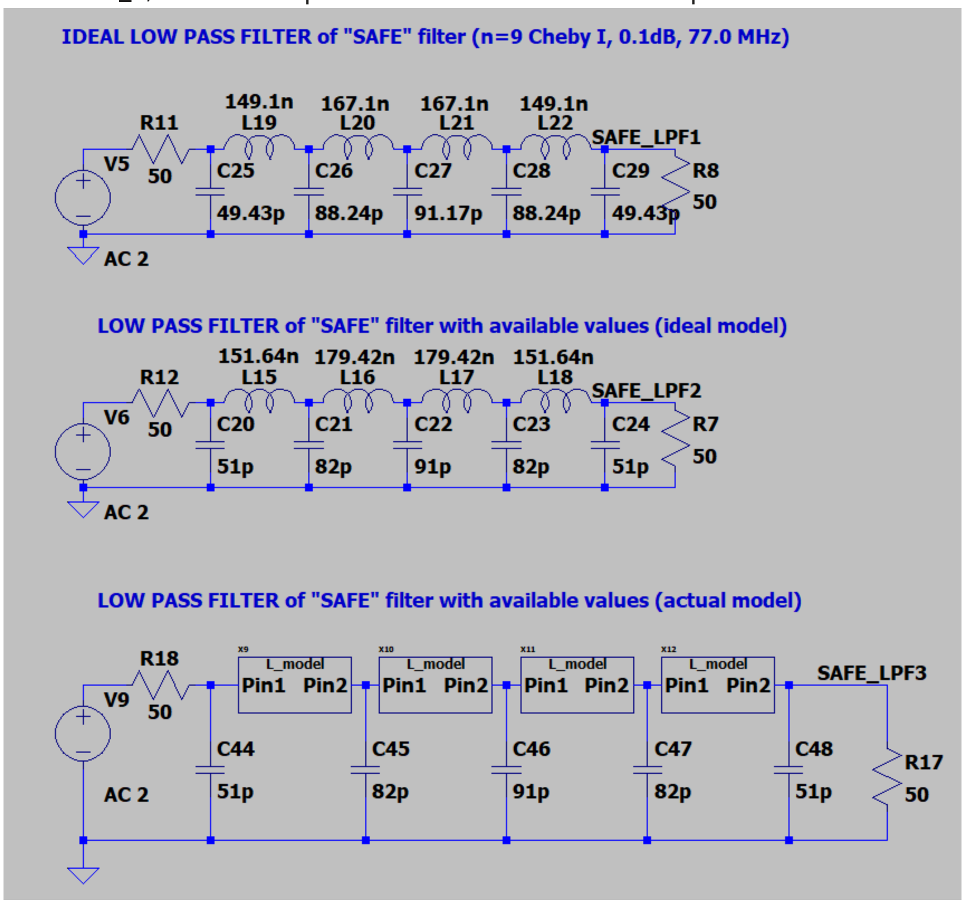

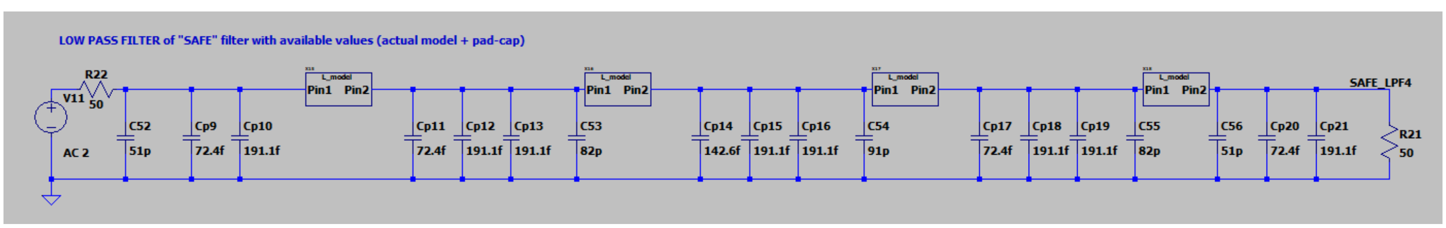

<u>Shunt capacitor modification based on pad-to-ground capacitance</u>

C used(pF)	Cpad_0805(pF)	Cpad_0402(pF)	Cpad_0603(pF)	New C(pF)	Available C(pF)
51	0.1911	0.0724	0.1426	50.74	51
82	0.1911	0.0724	0.1426	81.55	82
91	0.1911	0.0724	0.1426	90.48	91
82	0.1911	0.0724	0.1426	81.55	82
51	0.1911	0.0724	0.1426	50.74	51

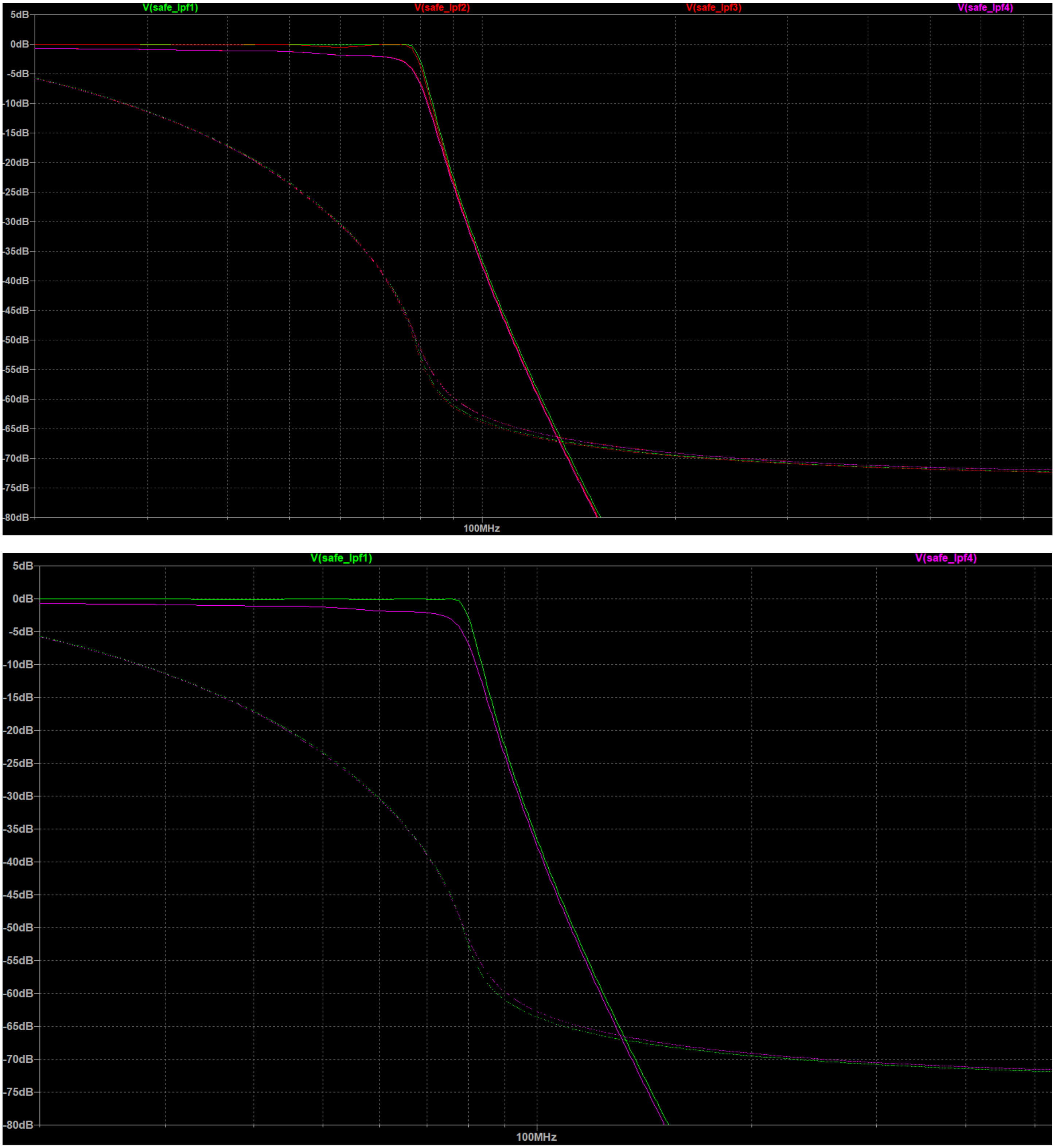

Figure A5: Comparison of SAFE_LPF_1 and SAFE_LPF4

c) Wide band filter response (Cascaded HPF and LPF)

- SAFE_BPF_1: Exact values, ideal components
- SAFE_BPF_2: available values, ideal components
- SAFE_BPF_3: available values, specific PN components, full models of inductors
- SAFE_BPF_4: like SAFE_BPE_3, but with capacitors added to model PCB pads.

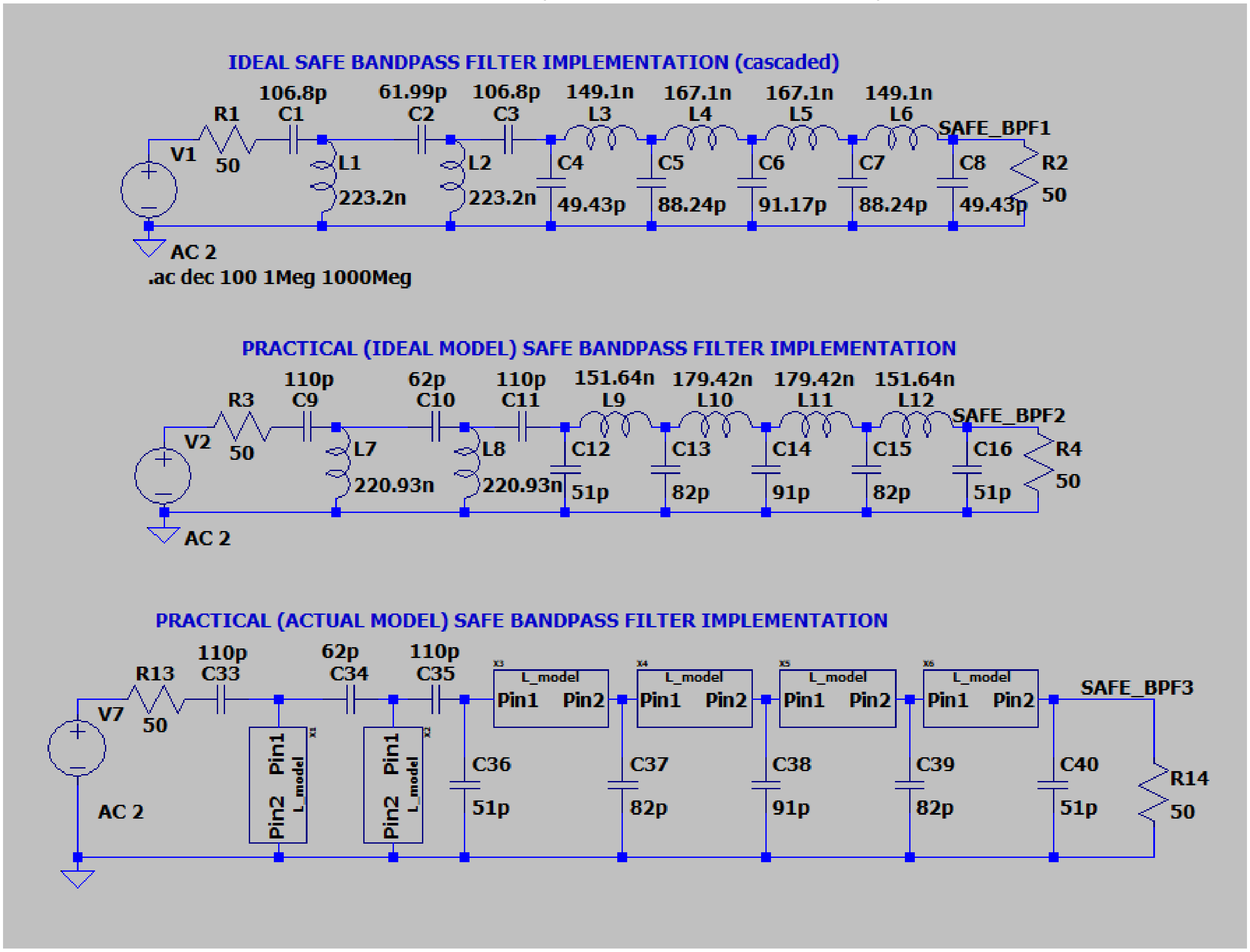

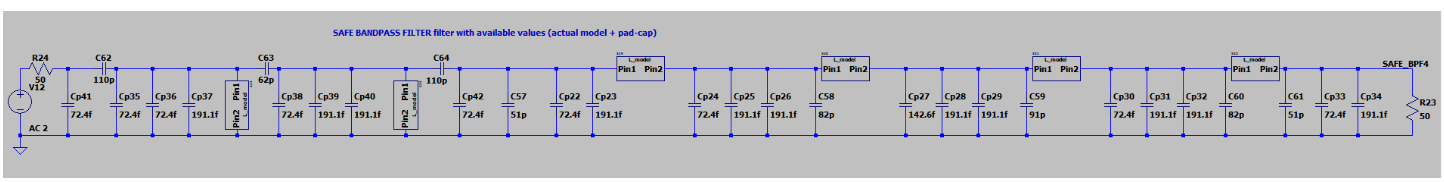

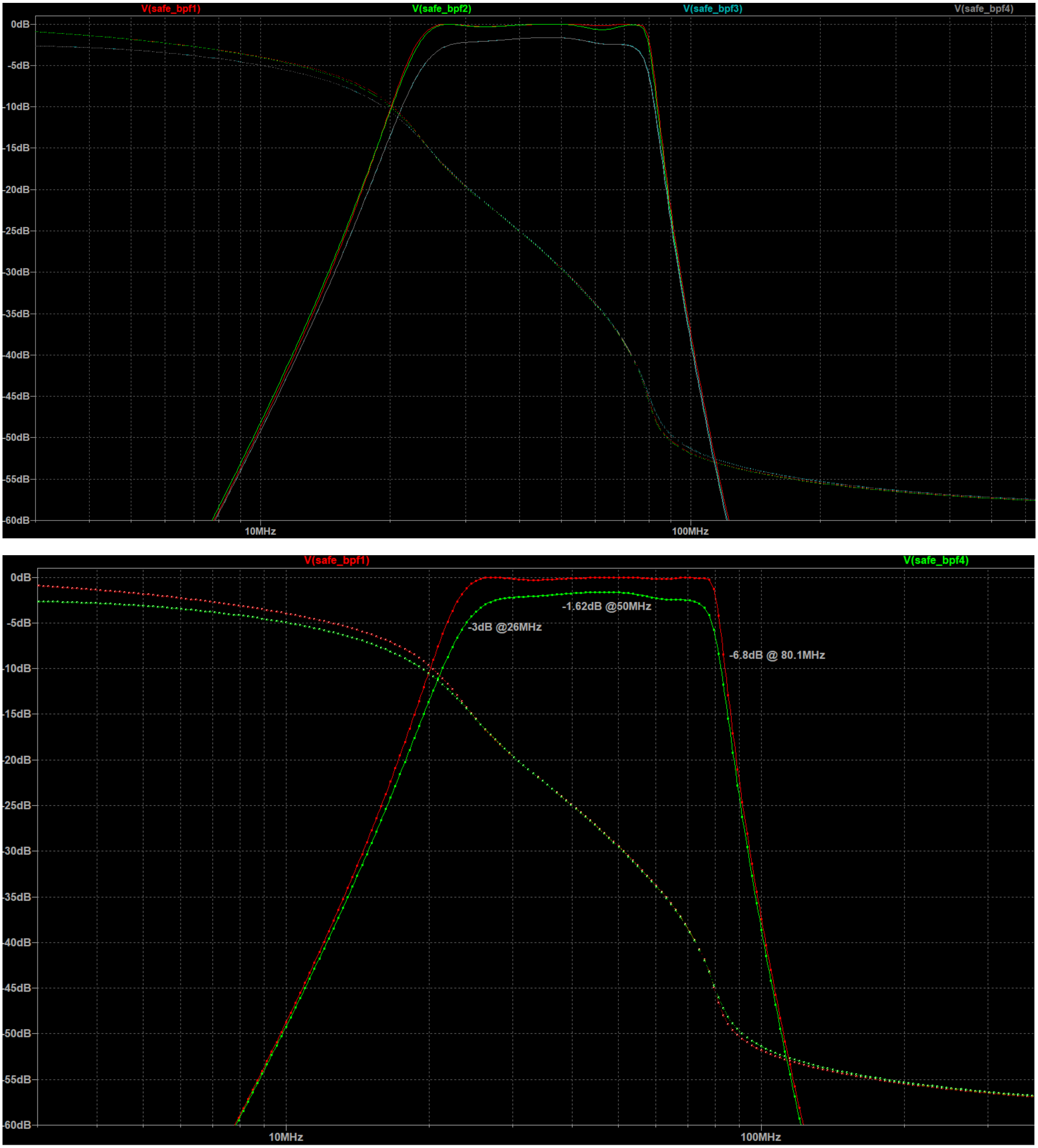

Figure A6: Comparison of SAFE_BPF_1 and SAFE_BPF4

III. Smooth filter implementation (n=7 Butterworth, 22.0 and 72.5 MHz)

- SMOOTH_BPF_1: Exact values, ideal components
- SMOOTH_BPF_2: available values, ideal components
- SMOOTH_BPF_3: available values, specific PN components, full models of inductors
- SMOOTH_BPF_4: like SMOOTH_BPE_3, but with capacitors added to model PCB pads.

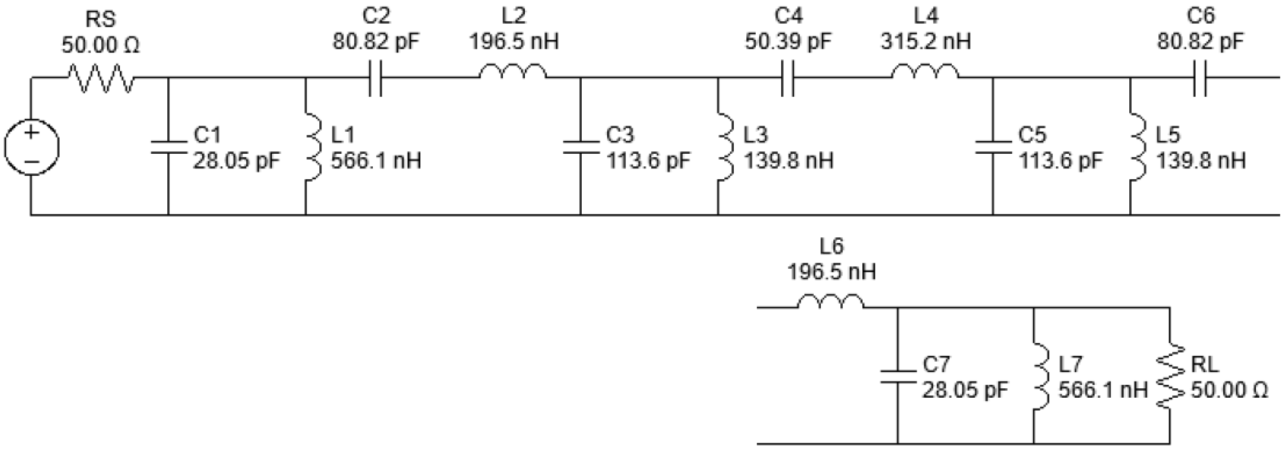

Figure 5. Smooth filter implementation.

S. No.	Filter exact value (pF)	Value used (pF)	MPN	Manufacturer	Tolerance	Voltage	Temp Coeff	Temp range	Package	Description	Variation
1	28.05	27	GRM1555C1H270FA01D	Murata	1	50	C0G, NP0	-55°C ~ 125'	0402	CAP CER 27PF 50V C0G/NP0 0402	3.7433155
2	80.82	82	GCM1555C1H820FA16D	Murata	1	50	C0G, NP0	-55°C ~ 125'	0402	CAP CER 82PF 50V C0G/NP0 0402	-1.460035
3	113.6	120	GRM1555C1H121FA01D	Kemet	1	50	C0G, NP0	-55°C ~ 125'	0402	CAP CER 120PF 50V C0G/NP0 0402	-5.633803
4	50.39	47	GRM1555C1H470FA01D	Murata	1	50	C0G, NP0	-55°C ~ 125'	0402	CAP CER 47PF 50V C0G/NP0 0402	6.7275253
5	113.6	100	GRM1555C1H101FA01D	Murata	1	50	C0G, NP0	-55°C ~ 125'	0402	CAP CER 100PF 50V C0G/NP0 0402	11.971831

S.No.	Filter exact value	L @ 50MHz (nH)	Manufacturer	Part number	R1 (ohm)	R2 (ohm)	C (pF)	L (nH)	k	(MHz)	% variation from	Nominal Inductance	L@f (MHhZ)	Tolerance	Q	Q@f (MHz)	DCR max	Irms(mA)	SRF(MHz)	Spice model input	Rtot @50 MHz
1	566.1	559.52	Coilcraft	0805HP-561	26	2.067	0.15	558.8	5.37E-04	1000	1.162339	560	100	2,5	39	50	2067	240	550	=0.0005374 C=0.15p R1=26 R2=2.067 L=558.8	3.80E+00
2	196.5	201.72		0603HP-R20	160	2	0.029	200	3.00E-04	2500	-2.65649	150	100	1,2,5	31	50	560	400	1150	K=0.0003 C=0.029p R1=160 R2=2 L=200n	2.12E+00
3	139.8	151.64		0805CS-151	24	0.56	0.11	149	2.23E-04	1500	-8.46924	150	100	1,2,5	31	50	560	400	1150	K=0.000223 C=0.11p R1=24 R2=0.56 L=149n	1.58E+00
4	315.2	325.32		0805CS-331	31	1.4	0.096	320	4.74E-04	1100	-3.21066	330	100	2,5	34	50	1400	310	650	K=0.000474 C=0.096p R1=31 R2=1.4 L=320n	3.35E+00

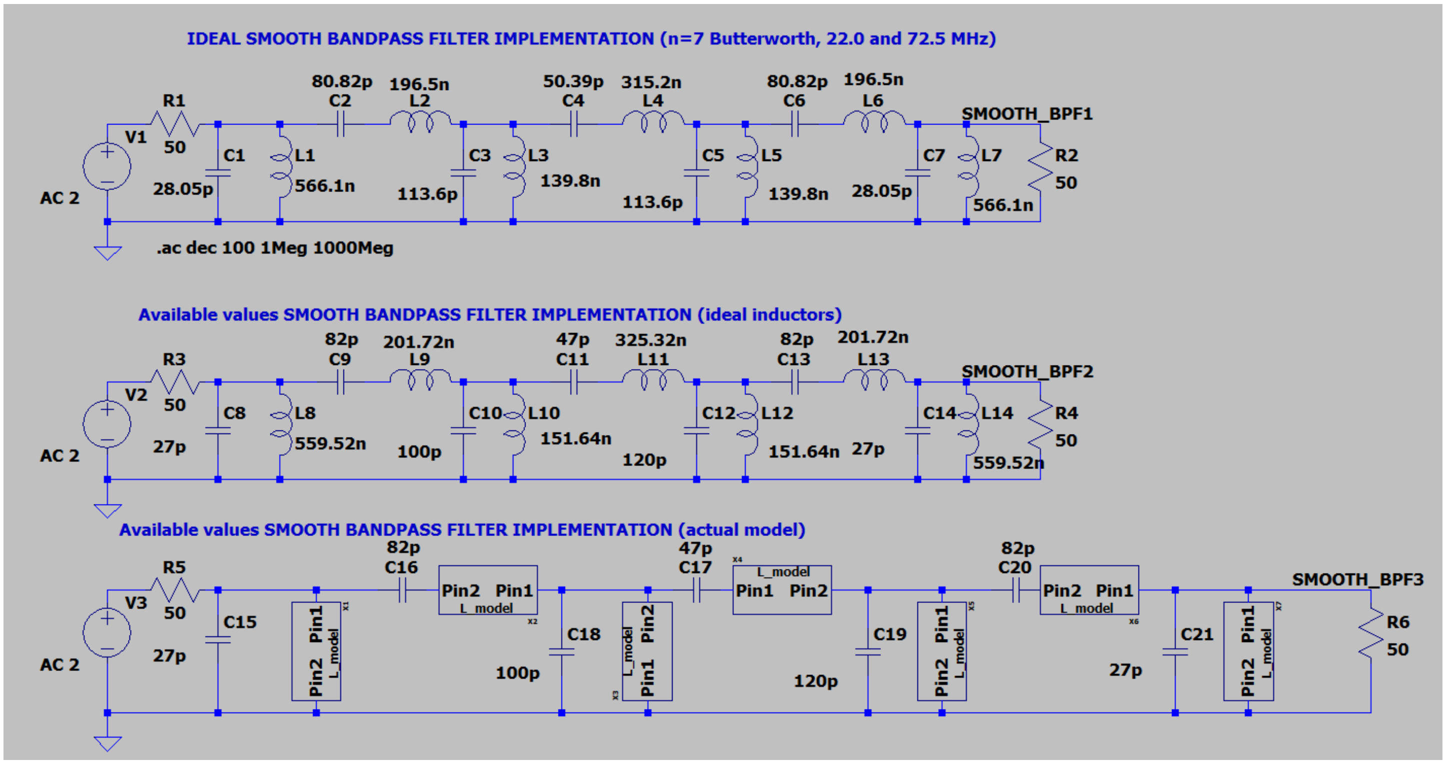
IDEAL SMOOTH BANDPASS FILTER IMPLEMENTATION (n=7 Butterworth, 22.0 and 72.5 MHz)
R1
50
V1
AC 2
C1
28.05p
L1
566.1n
80.82p
C2
196.5n
L2
C3
113.6p
L3
139.8n
50.39p
C4
315.2n
L4
C5
113.6p
L5
139.8n
80.82p
C6
196.5n
L6
C7
28.05p
L7
566.1n
SMOOTH_BPF1
R2
50
.ac dec 100 1Meg 1000Meg
Available values SMOOTH BANDPASS FILTER IMPLEMENTATION (ideal inductors)
R3
50
V2
AC 2
C8
27p
L8
559.52n
82p
C9
201.72n
L9
C10
100p
L10
151.64n
47p
C11
325.32n
L11
C12
120p
L12
151.64n
82p
C13
201.72n
L13
C14
27p
L14
559.52n
SMOOTH_BPF2
R4
50
Available values SMOOTH BANDPASS FILTER IMPLEMENTATION (actual model)
R5
50
V3
AC 2
C15
27p
82p
C16
C18
100p
47p
C17
C19
120p
82p
C20
C21
27p
SMOOTH_BPF3
R6
50
L_model
Pin1
Pin2

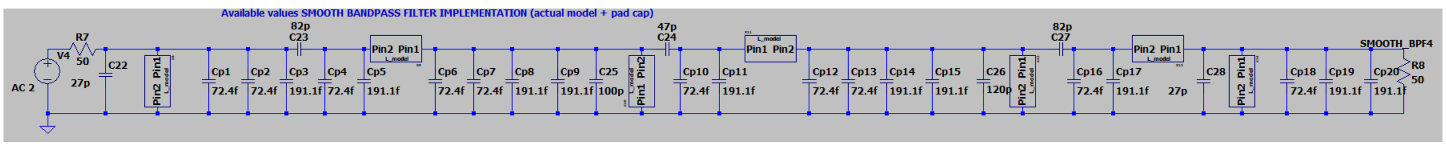
Available values SMOOTH BANDPASS FILTER IMPLEMENTATION (actual model + pad cap)
SMOOTH_BPF4

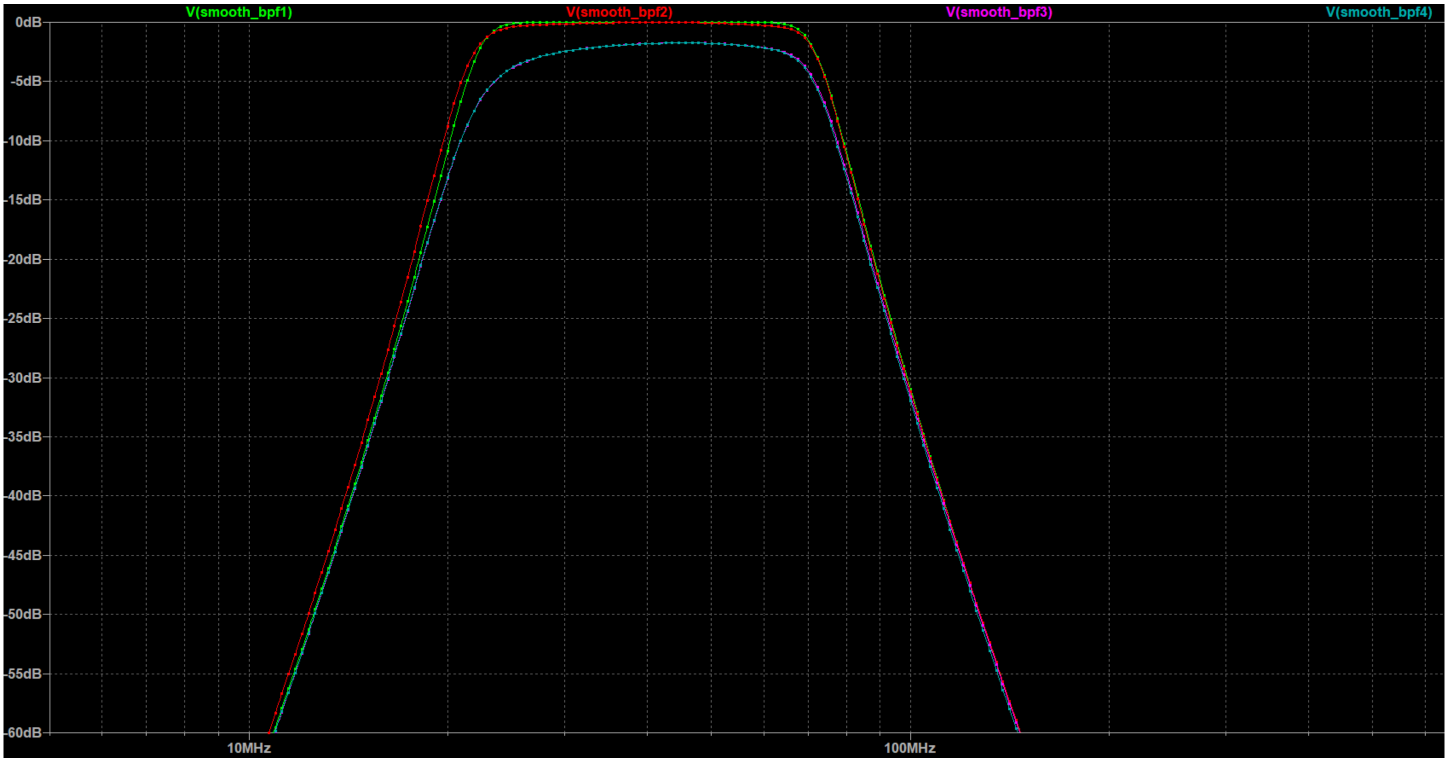

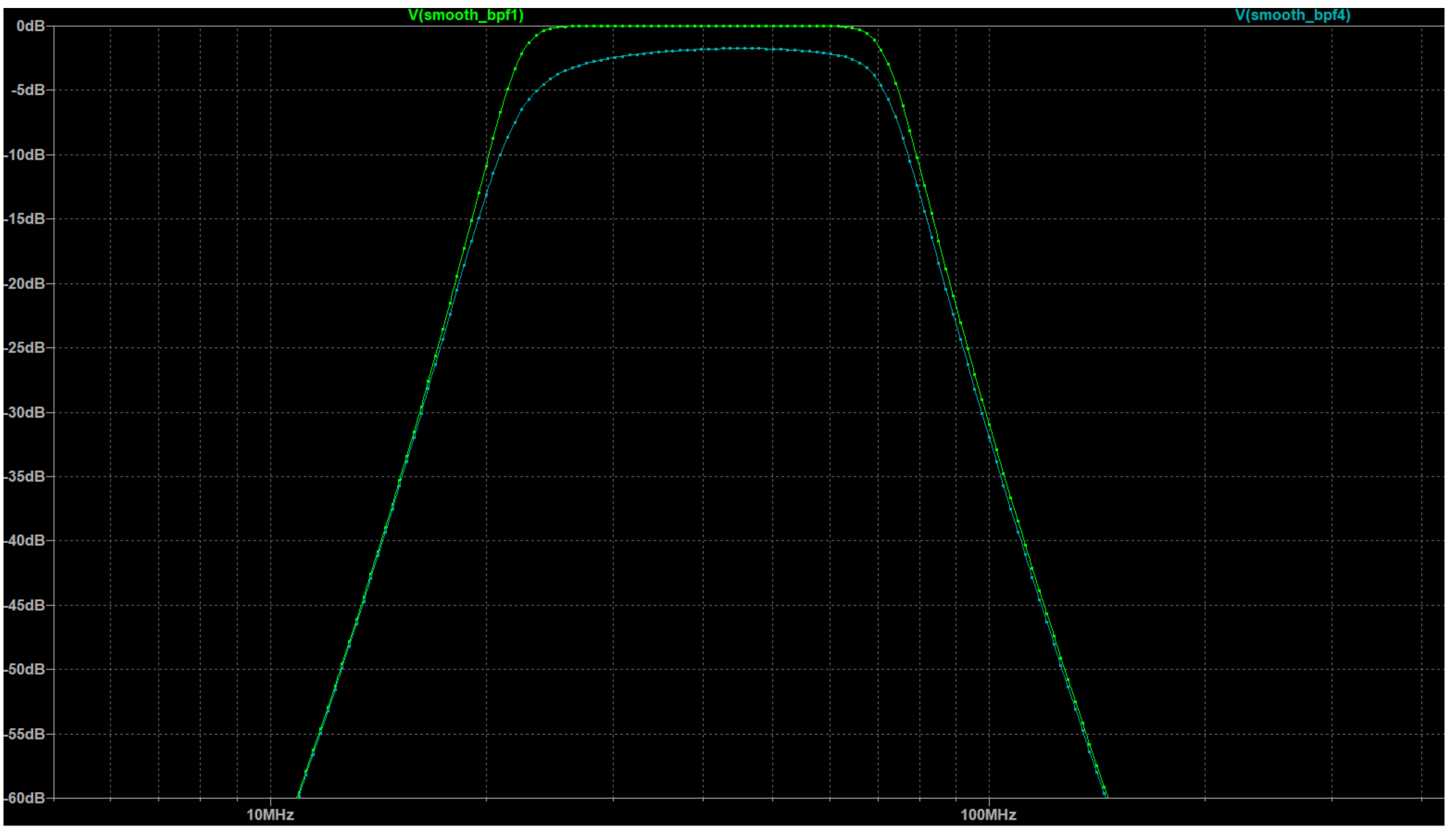

Figure A7: Comparison of SMOOTH_BPF_1 and SMOOTH_BPF4